Selective hydrometallurgical processing of NdFeB magnets: impact of roasting on leaching selectivity and impurity dissolution

Nicolas Stankovic, Jérôme Marin, Julien Jourdan, Thibault Quatravaux, Alexandre Chagnes

▶ **To cite this version:**

Nicolas Stankovic, Jérôme Marin, Julien Jourdan, Thibault Quatravaux, Alexandre Chagnes. Selective hydrometallurgical processing of NdFeB magnets: impact of roasting on leaching selectivity and impurity dissolution. Chemical Engineering Journal, 2026, 531, pp.174024. ⟨10.1016/j.cej.2026.174024⟩. ⟨hal-05511282⟩

HAL Id: hal-05511282

https://hal.univ-lorraine.fr/hal-05511282v1

Submitted on 14 Feb 2026

HAL is a multi-disciplinary open access archive for the deposit and dissemination of scientific research documents, whether they are published or not. The documents may come from teaching and research institutions in France or abroad, or from public or private research centers.

L'archive ouverte pluridisciplinaire **HAL**, est destinée au dépôt et à la diffusion de documents scientifiques de niveau recherche, publiés ou non, émanant des établissements d'enseignement et de recherche français ou étrangers, des laboratoires publics ou privés.

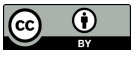

Distributed under a Creative Commons CC BY 4.0 - Attribution - International License

Chemical Engineering Journal 531 (2026) 174024

Contents lists available at ScienceDirect

Chemical Engineering Journal

journal homepage: www.elsevier.com/locate/cej

Selective hydrometallurgical processing of NdFeB magnets: impact of roasting on leaching selectivity and impurity dissolution☆

Nicolas Stankovic [a,b], Jérôme Marin [a], Julien Jourdan [b], Thibault Quatravaux [b], Alexandre Chagnes [a,*]

[a] University of Lorraine, CNRS, GeoRessources, F-54000, Nancy, France
[b] University of Lorraine, CNRS, Institut Jean Lamour, F-54000, Nancy, France

ARTICLE INFO

Keywords:
Rare-earth elements
Leaching
Thermal treatment
Magnet
Decrepitation
Recycling
Hydrometallurgy

ABSTRACT

This study addresses the hydrometallurgical recycling of NdFeB magnets obtained from discarded hard disk drives. Magnet powders processed via hydrogen decrepitation were thermally oxidized at 850 °C to convert iron into insoluble oxides, minimizing iron dissolution during subsequent acid leaching. The research examined various parameters and different inorganic and organic acids – acetic, citric, trichloroacetic, methanesulfonic, and hydrochloric acids – to identify suitable operating conditions for rare-earth elements (REE) recovery. Thermal pretreatment substantially improved iron selectivity but initially limited REE extraction. Elevated temperatures notably enhanced leaching performance since hydrochloric acid (HCl) at 93 °C achieved complete dissolution of REEs with minimal iron contamination. Effective leaching conditions (0.5 mol/L HCl, solid-to-liquid ratio S/L = 100 g/L, 93 °C, 8 h) were established, yielding high-purity solutions suitable for selective extraction. In addition to REEs, the dissolution behavior of other potentially valuable elements such as boron, cobalt, aluminum, and copper was also assessed, providing insights into their co-recovery potential. The resulting leachate composition, characterized by high REE concentrations and limited impurity levels, offers favorable conditions for implementing solvent extraction processes for the selective recovery of both REE and the other critical metals contained in the leachate.

1. Introduction

Neodymium–iron–boron (NdFeB) magnets have become essential to numerous modern technologies, driving a significant rise in demand for key rare earth elements (REEs) such as neodymium (Nd), praseodymium (Pr) and dysprosium (Dy). Since their development, the demand for these critical materials has escalated notably. According to a report from the European Commission's Joint Research Centre, in 2018, global consumption of these REEs was around 50,000 tons, with Nd making up about 40,000 tons [1]. Looking ahead, the International Renewable Energy Agency anticipates a dramatic increase in demand, projecting annual needs could reach approximately 225,000 tons. This growth is predominantly driven by expanding production in the electric vehicle sector (approximately 180,000 tons) and rising installations in wind energy technology (around 50,000 tons) [2]. Such an unprecedented surge may result in a substantial shortfall of nearly 135,000 tons of NdFeB magnets within the coming decade. To mitigate this impending shortage, efforts are concentrated on both developing new mining operations and enhancing recycling practices. Several new mining projects are currently underway or planned in regions with potential reserves, including Canada, Australia, Turkey, and the Nordic countries. However, reliance solely on primary extraction might not sufficiently meet the future needs. Therefore, many governments, especially in regions with limited mining capacity like Europe, the United States, and Japan, have increased investments in the recycling sector to improve the security of REE supplies [1,3]. Although current recycling rates are relatively low, substantial room exists for expansion, potentially reclaiming up to 2500 tons of essential elements such as Nd and Dy annually [3]. The critical role of recycling NdFeB magnets stems from their unparalleled magnetic properties, identified since their introduction in 1983. Compared to traditional magnet types, NdFeB magnets provide remarkably higher magnetic energy densities – approximately fifteen-

☆ This article is part of a Special issue entitled: 'ICSET2025' published in Chemical Engineering Journal.

* Corresponding author.
E-mail address: alexandre.chagnes@univ-lorraine.fr (A. Chagnes).

https://doi.org/10.1016/j.cej.2026.174024
Received 9 September 2025; Received in revised form 13 January 2026; Accepted 10 February 2026
Available online 10 February 2026
1385-8947/© 2026 The Authors. Published by Elsevier B.V. This is an open access article under the CC BY license (http://creativecommons.org/licenses/by/4.0/).

fold that of ferrite-based magnets, seven-fold that of AlNiCo magnets, and roughly two and a half times greater than samarium-cobalt magnets [1]. Such exceptional attributes have made NdFeB magnets vital components in advanced technology fields dominating over half of the global permanent magnet market [4]. NdFeB magnets typically contain iron (60–70 wt%), neodymium (20–25 wt%), boron (around 1 wt%), and smaller proportions of praseodymium and dysprosium (each up to 5 wt%), which contribute to improved thermal stability at operating temperatures as high as 200 °C. Additionally, the inclusion of trace elements such as cobalt, copper, and nickel further enhances the magnets' performance and durability [1].

In response to environmental concerns and increasing demand for NdFeB magnets, innovative recycling methods aligned with circular economy principles have emerged (Fig. 1). A particularly promising approach is short-loop recycling (Fig. 1, route a), involving hydrogen decrepitation (HD). In this process, hydrogen induces brittleness in spent magnets, breaking them down into powders suitable for new magnet fabrication through magnetic compaction and high-temperature sintering [5]. An advanced variant, the Hydrogenation Disproportionation Desorption Recombination (HDDR) process, provides further refinement by hydrogenating both grain boundary phases and the $Nd_2Fe_{14}B$ matrix, followed by a high-temperature disproportionation reaction and subsequent desorption of hydrogen. The final recombination at elevated temperatures restores the original $Nd_2Fe_{14}B$ magnetic phase [6–12]. HD also serves as an efficient pre-treatment for longer-loop recycling processes, facilitating subsequent extraction of REEs through hydrometallurgical or pyrometallurgical techniques [13–17]. In pyrometallurgy, another innovative method, Liquid Metal Extraction (Fig. 1, route c), selectively recovers REEs from magnet scrap using molten magnesium [18,19]. In this technique, magnets are immersed in liquid magnesium, allowing REEs to diffuse into the molten metal, followed by distillation to separate metallic rare earths. The process significantly reduces environmental impact compared to traditional mining by virtually eliminating effluent. Magnesium is reusable after distillation, and iron-rich residues can re-enter steel manufacturing, highlighting the method's economic and ecological advantages despite its relatively high energy requirements.

A more conventional recycling method, the hydrometallurgical approach (Fig. 1, route b), involves several sequential steps, including leaching, solvent extraction, ion exchange, and precipitation, to recover REEs. These steps are similar to techniques commonly applied in hydrometallurgical ore processing and have been extensively studied to optimize efficiency and minimize environmental impacts [20]. Thermal oxidative pre-treatment enhances the selectivity during leaching by preventing iron (Fe) dissolution, crucial since iron contamination complicates REE purification during subsequent extraction and precipitation steps. After extraction, REEs are precipitated as salts, subsequently converted into pure metals for new magnet production. Additionally, this method can co-recover other valuable metals such as Pr, Dy, Ni, Co, and Cu, further promoting resource efficiency, while residual Fe can be recycled into the steel industry.

Extensive research has been conducted on hydrometallurgical recycling methods for recovering REEs from NdFeB magnets, primarily focusing on leaching processes using inorganic and organic acids. Early investigations, such as those by Lyman and Palmer [21], demonstrated that sulfuric acid effectively dissolves magnet scrap, selectively leaching REEs while preventing excessive iron oxidation under mild conditions. Subsequent work by Rabatho et al. [22] utilized nitric acid with hydrogen peroxide to achieve efficient dissolution of Nd, Dy and B, significantly reducing Fe dissolution at lower acid concentrations.

Additional studies, including those by Yoon et al. [23] and Hoogerstraete et al. [24], underscored the significance of thermal oxidative pretreatment in enhancing selective dissolution. Yoon et al. effectively combined roasting with sulfuric acid leaching, achieving complete Nd extraction at elevated temperatures, whereas Hoogerstraete et al. employed oxidative roasting at higher temperatures followed by hydrochloric acid leaching, yielding high purity REE solutions with minimal iron contamination. More recently, Kumari et al. [25] optimized

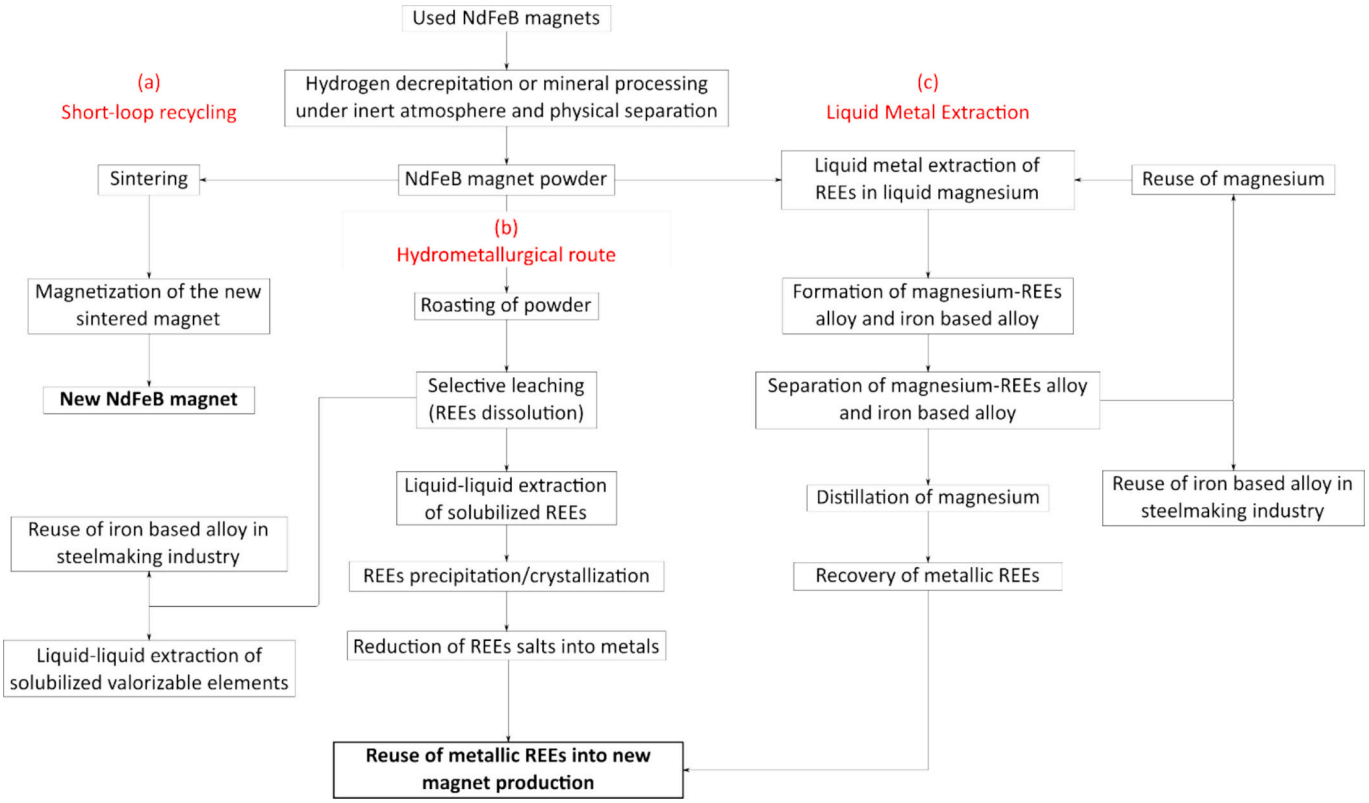

Fig. 1. Recycling routes of REEs from NdFeB magnets, (a) short-loop recycling, (b) hydrometallurgical route, (c) liquid metal extraction (pyrometallurgy).

pre-treatment conditions, including demagnetization and roasting at 850 °C, significantly improving REE dissolution efficiencies with very limited iron contamination, thus simplifying downstream purification processes. Similarly, Parhi et al. [26] and Erust et al. [27] reported high dissolution yields using dilute hydrochloric and sulfuric acids, respectively, albeit highlighting persistent challenges with iron dissolution.

Parallel to inorganic acid research, growing environmental concerns have driven interest toward organic acid leaching methods. Yoon et al. [23] demonstrated effective selective leaching of Nd and Dy with acetic acid following combined mechanical and thermal treatments, limiting iron dissolution significantly. Behera and Parhi [28] confirmed high Nd dissolution efficiencies with acetic acid under optimized conditions, though significant iron co-dissolution persisted at higher acid concentrations. Investigations by Gergoric et al. [29,30] and Reisdörfer et al. [31] compared various organic acids, such as citric, malic, glycolic, and maleic acids, achieving high REE extraction efficiencies but frequently encountering iron contamination issues, especially at prolonged leaching times or higher acid concentrations. Recent studies by Belfqueh et al. [32] systematically evaluated several organic acids, reaffirming higher acetic acid performance in terms of selective REE recovery compared to citric, tartaric, and formic acids.

However, the current literature often overlooks the behavior of non-rare earth elements co-present in the leached material, such as aluminum (Al), boron (B), cobalt (Co), and iron (Fe). Understanding their solubility, co-dissolution, and potential for recovery or removal is crucial, as their presence can significantly impact downstream purification processes, material purity, and overall environmental performance. A more comprehensive assessment of these co-elements is therefore needed to improve process control and support the development of truly sustainable recycling workflows.

In this context, the present work primarily aims at investigating the dissolution behavior of non-REE elements during the leaching of HD powders derived from NdFeB magnets, using organic and inorganic acids. However, such an analysis is only meaningful under conditions where REE dissolution is ensured, as the absence of efficient REE recovery would prevent any economically viable recycling process.

To this end, a preliminary roasting treatment was applied to oxidize the HD powder, effectively converting iron into insoluble oxides in the leaching media, as demonstrated previously by Kumari et al. [25] and Reisdörfer et al. [31] Establishing effective and selective REE leaching conditions was therefore a necessary prerequisite to define a robust and process-relevant baseline. Once these conditions were achieved, particular attention was given to the dissolution behavior of co-existing elements, an aspect that remains insufficiently addressed in the literature under conditions representative of an economically viable and selective recycling process.

By explicitly examining the behavior of both target REEs and accompanying elements, this study provides new insights into impurity management, co-element valorization, and the design of selective hydrometallurgical flowsheets. This comprehensive approach supports the principles of green chemistry and circular economy by promoting resource efficiency, minimizing environmental impact, and enabling the full valorization of end-of-life products.

2. Materials and methods

2.1. Experimental procedures

2.1.1. Sample preparation

Permanent NdFeB magnets recovered from discarded hard disk drives (HDDs) were processed into powder using the hydrogen decrepitation (HD) method at room temperature under a hydrogen pressure of 1 bar. The resulting material was then sieved to isolate particles smaller than 200 μm, yielding a median particle size (d_{50}) of 100 μm. Assuming a Rosin–Rammler [33,34] particle size distribution with a shape parameter $n = 2.5$, consistent with previous work [19] on decrepitated NdFeB powders, the corresponding D_{10} and D_{90} were model-based estimates equal to 47 μm and 158 μm, respectively. The results of ICP-MS analysis performed on the decrepitated powder are presented in Table 1. Prior to elemental analysis, solid samples were subjected to total acid digestion. Approximately 50 mg of dried powder were weighed into Teflon vessels and treated with 10 mL of freshly prepared aqua regia ($HCl:HNO_3 = 3:1$ *v*/v). The suspensions were heated on a hot plate at 120 °C for 2 h until complete dissolution. This digestion procedure is consistent with established protocols for NdFeB magnets and rare-earth–rich materials using aqua regia or mixed HCl/HNO_3 systems. After cooling, the solutions were quantitatively transferred and diluted to a final volume of 50 mL with deionized water, and filtered when necessary before analysis. Iron was quantified by ICP-OES due to its higher concentration, while other elements were determined by ICP-MS. [35,36]

2.1.2. Thermal oxidation of the HD powder as pre-treatment

Prior to the leaching experiments, the HD magnet powder underwent a roasting process aimed at oxidizing the material, specifically converting iron into oxides that are insoluble in the leaching media, as demonstrated by Kumari [25] and Gergoric [30]. Gergoric conducted roasting at 400 °C for 1.5 h, while Kumari employed a higher temperature of 850 °C for 6 h. To establish effective roasting conditions for complete oxidation of the HD powder and to enhance leaching selectivity by rendering iron insoluble, an initial oxidation study was carried out on 3 g of HD powder using TGA-DSC (Setaram – TG96) at 450 °C and 850 °C for 14.5 h under an air flow of 200 $mL{\cdot}min^{-1}$. Based on the results, full oxidation was then performed in a muffle furnace (Nabertherm N 11/H, maximum temperature 1280 °C). The mass change was assessed by weighing the sample in a crucible before and after roasting.

2.1.3. Leaching of the oxidized powder

During the roasting process, the samples agglomerated and were subsequently pulverized using a micro-crusher to achieve a particle size below 100 μm that is appropriate for ensuring efficient dissolution. [28] Since laser granulometry was not available, its particle size distribution was estimated using a Rosin–Rammler [33,34] model with the same shape parameter ($n = 2.5$) previously used for the <200 μm powder. Assuming $D_{50} = 60$ μm as typical median size of such micro-crushing conditions, the model predicts $D_{10} = 29$ μm and $D_{90} = 89$ μm. These values indicate that the <100 μm micro-crushed fraction presents a relatively narrow and homogeneous particle size distribution. [19]

Leaching experiments were performed in 150 mL beakers containing 100 mL of leaching solution. Stirring was maintained throughout the process using a magnetic heating and stirring plate. The acids employed for leaching included acetic acid (puriss p.a. >99.8%, Sigma Aldrich), citric acid (ACS reagent >99.5%, Sigma Aldrich), trichloroacetic acid (ACS reagent >99.0%, Sigma Aldrich), methanesulfonic acid (>99.0%, Sigma Aldrich), and hydrochloric acid (puriss p.a. >37.0%, Sigma Aldrich). Leaching solutions were prepared by diluting concentrated acids to the desired concentrations using ultrapure water with a resistivity of 18.2 MΩ.cm at 25 °C and an ionic content of less than 1 μg/L.

Table 1
Elemental analysis of the decrepitated powder of spent magnets.

Elements	Contents (%)	Uncertainties (%)
Fe	64.05	< 2%
Nd	23.34	< 5%
Dy	3.26	< 5%
Pr	1.73	< 5%
Gd	1.35	< 5%
Co	1.01	< 5%
B	1.00	< 5%
Al	0.68	< 10%
Ge	0.23	< 10%
Cu	0.16	< 10%
Nb	0.11	< 10%
Ga	0.11	< 10%

This water was produced using a Direct-Q® 3 UV Remote Water Purification System equipped with a 0.22 µm filter.

Initial leaching experiments followed the procedure described by Gergoric [30], which involved using 1 mol/L acid, stirring at 400 rpm, a temperature of 23 ± 1 °C, a solid-to-liquid (S/L) ratio of 20 g/L, and a leaching duration of 24 h. The mass of the powder was accurately measured prior to leaching using a precision balance (Ohaus PR Series, model PR223) to enable calculation of leaching efficiency.

Leaching effiency of the element (i) was determined using the following equations:

$$Leaching\ effiency_i(\%) = \left(\frac{Amount\ of\ (i)\ in\ the\ leachate}{Initial\ amount\ of\ (i)\ in\ the\ powder}\right) \times 100 = \left(\frac{n_{i,PLS}}{n_{i,powder}}\right) \times 100$$

$$Leaching\ effiency_i(\%) = \left(\frac{C_{i,PLS}\ \mathrm{x}\ V_{PLS}}{(C_{powder}(i)\ \mathrm{x}\ m_{powder})}\right) \times 100$$

where $n_{i,PLS}$ (mol) corresponds to the amount of element i in the pregnant leach solution (PLS), and $n_{i,powder}$ (mol) is the initial amount of i present in the roasted powder. The term $C_{i,PLS}$ (mg.L^{-1}) refers to the concentration of element i in the leachate, while V_{PLS} (L) denotes the total volume of the pregnant leach solution collected after leaching. $C_{powder(i)}$ (mg.g^{-1}) represents the initial content of element i in the roasted powder, expressed per gram of solid, and m_{powder} (g) is the total mass of powder subjected to leaching. Both formulations are equivalent and can be employed depending on whether the available data are expressed in terms of molar quantities or concentrations.

Several parameters were investigated to determine favorable conditions and better understand the leaching behavior of REEs, including roasting time, acid concentration, addition of chloride ions, type of organic acid, acid renewal, use of inorganic acids, and temperature.

2.1.4. Liquid-liquid extraction post-processing

Liquid-liquid extraction have been performed by using the pregnant liquor solution made by leaching HD powder roasted at 850 °C during 6 h under the following experimental conditions: HCl at 0.5 mol/L, S/L = 100 g/L, temperature = 93 °C, agitation = 500 rpm. To perform liquid-liquid extraction experiments, 50 mL of the pregnant liquor solution were contacted with the extraction solvent in centrifuge tubes (the volume of the extraction solvent depends on the phase volume ratio O/A). The organic solvent was made of di(2-ethylhexyl)phosphoric acid (D2EHPA) (Sigma Aldrich) and tributyl phosphate (TBP) (Sigma Aldrich) diluted in Kerosene (low odor, Thermo Scientific) to the desired concentration. Tubes were placed in a shaker (Laboshake Gerhardt Analytical Systems model LS500) for shaking at 250 rpm during 30 min at a temperature of 25 °C to reach the steady state. After shaking, tubes were centrifuged at 2000 rpm during 2 min (Unrefrigerated benchtop centrifuge Sigma model 3-16 L) to separate the aqueous solution and the extraction solvent. The aqueous solution is then recovered and diluted 100 times for elemental analyses.

The extraction rates are calculated using the following equation:

$$Extraction\ rate\ (\%) = \left(1 - \frac{n_{aq,ext}}{n_{aq,0}}\right) \mathrm{x}\ 100 = \left(1 - \frac{C_{aq,ext}}{C_{aq,0}}\right) \mathrm{x}\ 100$$

Where $C_{aq,0}$ and $n_{aq,0}$ represent the initial concentration and initial amount of substance in the aqueous phase, respectively, while, $C_{aq,ext}$ and $n_{aq,ext}$ correspond to the concentration and amount of substance after extraction in the aqueous phase.

2.2. Characterization of the materials

2.2.1. X-ray diffraction spectroscopy

Following the roasting and leaching experiments, both the treated powder and leach residues were recovered, dried, and subjected to X-ray diffraction (XRD) analysis. XRD patterns were acquired using a Bruker D8 Discover diffractometer equipped with a Cu-Kα$_1$ radiation source (λ = 1.5406 Å), operating at 40 kV and 40 mA. Measurements were performed under ambient conditions using a LynxEye detector, with data collected over a 2θ range of 2.5° to 65°, at a step size of 0.035°, and a counting time of 3 s per step. Phase identification was carried out using Match! 4 software, with diffraction peaks matched against the integrated powder diffraction database provided within the software.

2.2.2. Microwave plasma atomic emission spectrometer

At scheduled intervals during the leaching process, 3 mL liquid samples were collected using a volumetric pipette. These samples were immediately filtered under vacuum through 0.45 µm hydrophilic membranes to remove any residual solids. The pH of the filtrates was then measured using a VWR® pHenomenal® pH 1100 L meter. Prior to use, the pH electrode was calibrated with four buffer standards (pH 4, 7, 9, and 10; VWR Chemicals). The redox potential (Eh vs. Ag/AgCl) was measured using a VWR® pHenomenal® Redox 110 L meter equipped with a pHenomenal® Redox electrode calibrated with a standard redox potential solution at 400 mV vs Ag/AgCl (VWR Chemicals), as recommended by the manufacturer. Following filtration, each sample was diluted 100-fold with deionized water (resistivity = 18 Mohms, VWR Puranity TU 6+) and acidified with 2% HNO_3 (puriss p.a. >65%, Sigma Aldrich) to ensure sample stability before elemental analysis. Metal concentrations in the resulting solutions were quantified using a Microwave Plasma–Atomic Emission Spectrometer (MP-AES, Agilent 4210). To enable quantitative multi-element analysis, a mixed-element stock solution was prepared to reflect the elemental composition at the S/L ratio used in leaching experiments. From this stock, a set of eight calibration standards was prepared, covering a concentration range from 0.08% to 125% relative to the initial composition. For each element (excluding Nb), two to six emission lines were monitored to validate concentration measurements. In addition, individual elemental standard solutions at 75% of the expected concentration were prepared to support Fast Linear Interference Correction (FLIC), utilizing MP-Expert software for data processing. All calibration and standard solutions were freshly prepared for each analytical session, with final concentrations adjusted to match the specific elemental distribution of the leaching feedstock.

3. Results and discussion

3.1. Powder thermal oxidation and effect of roasting time on leaching

3.1.1. Thermal oxidation of the HD powder

The primary objective of the roasting step was to render iron insoluble by converting it into hematite (Fe_2O_3), a phase known for its limited solubility in acidic media, while simultaneously oxidizing the Nd–Fe–B intermetallic matrix into rare-earth–containing oxides such as $NdFeO_3$. This transformation is intended to suppress iron dissolution during subsequent leaching of NdFeB magnet powder. Two established roasting protocols were considered: one based on Kumari's method [25], which applies a high-temperature treatment at 850 °C for 6 h, and another derived from Gergoric's [30] study, involving a lower temperature of 400 °C for 1.5 h. While Kumari reported improved selectivity during leaching, Gergoric's results showed no significant distinction in element recovery. To further investigate the influence of temperature and duration on iron oxidation and its impact on leaching behavior, roasting trials were conducted on HD powder at 450 °C and 850 °C for an extended period of 14 h. The resulting mass changes, shown in Fig. 2 (a), reflect the oxidation progression at 450 °C (blue line) and 850 °C (red line) while DTG curves are given in Fig. 2(b) for better understanding of the thermal chemical behavior. At 450 °C, oxidation appeared to be ongoing even after 14 h, as indicated by a mass increase of 17.25%.

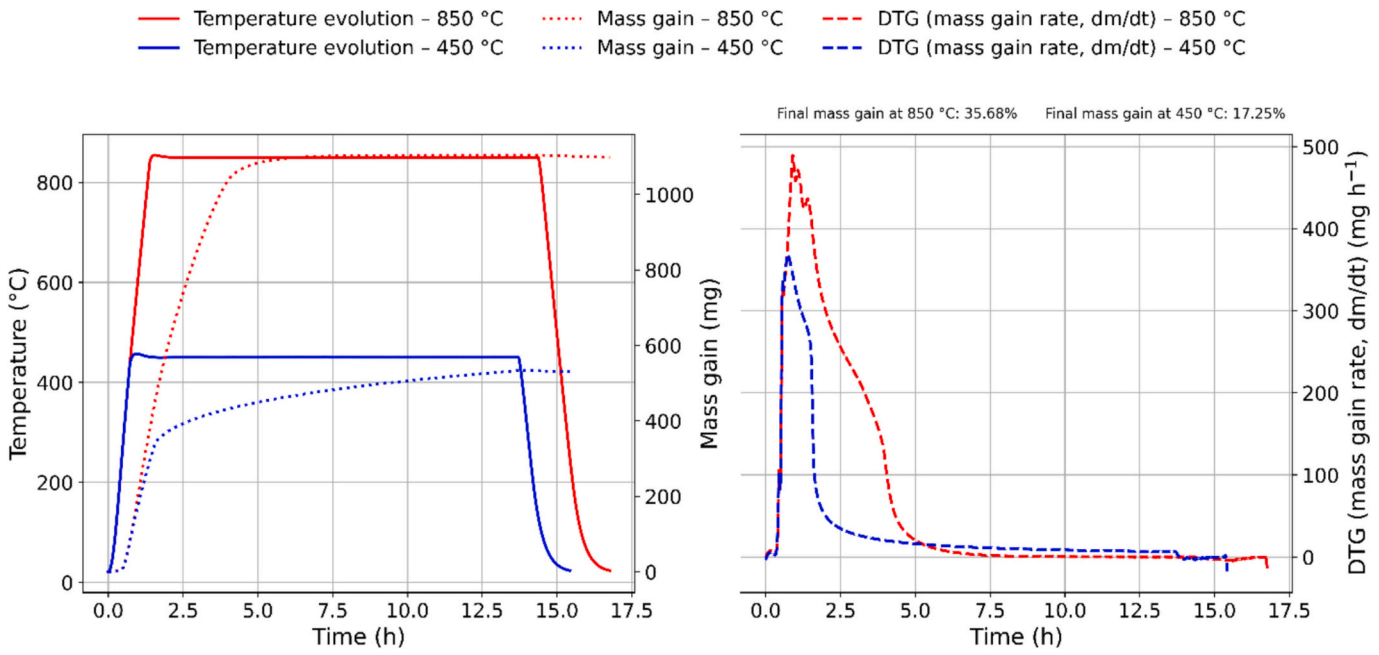

Fig. 2. TGA-DSC analysis of HD powder under air at 850 °C (red) and 450 °C (blue).

Fig. 3 presents the X-ray diffraction (XRD) patterns of HD magnet powder subjected to roasting at 850 °C for 1, 2, and 6 h.

In contrast, roasting at 850 °C led to a clear mass stabilization after approximately 6 h, with a final mass gain of 35.68%, confirming full oxidation, in agreement with earlier findings by Kumari. To assess how roasting duration affects the selectivity of the leaching process, additional samples were treated in a muffle furnace at 850 °C for varying durations of 1, 2, and 6 h. Each sample was placed in a crucible and

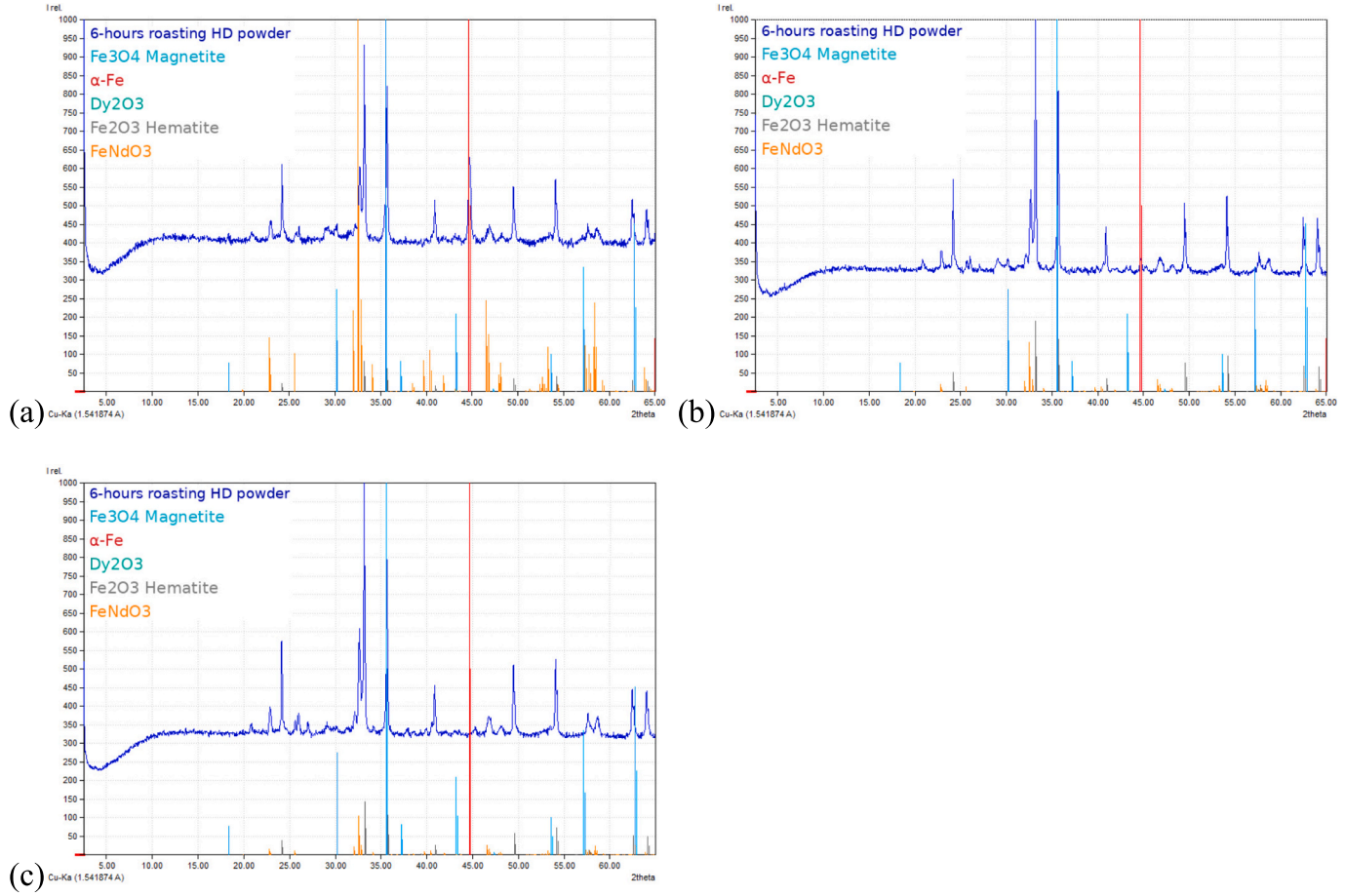

Fig. 3. XRD patterns of roasted powders after (a) 1-h, (b) 2-h and (c) 6-h.

subjected to thermal treatment under ambient air conditions.

Compared to the untreated powder, the roasted samples exhibit distinct changes in crystalline phases, highlighting the progressive transformation induced by thermal oxidation. In all roasted samples, diffraction peaks corresponding to hematite (Fe_2O_3) are clearly observed, becoming more pronounced with longer treatment times. The formation of neodymium orthoferrite ($NdFeO_3$) is also evident across all durations, with relatively consistent peak intensities. This phase is likely the result of oxidation of the $Nd_2Fe_{14}B$ structure. A metallic iron phase (α-Fe) is detected primarily in the sample roasted for 1 h, with its intensity decreasing after 2 h and disappearing entirely after 6 h. This disappearance indicates the progressive oxidation of metallic iron into more stable oxide phases, namely Fe_2O_3 and $NdFeO_3$. Additionally, minor peaks attributed to magnetite (Fe_3O_4) are detected, becoming more distinct in samples treated for longer durations. Dysprosium oxide phases are consistently present in all oxidized powders, regardless of roasting time, suggesting that Dy oxidation occurs readily and remains stable under the tested conditions.

These structural transformations were targeted based on prior literature to enhance selectivity during further leaching by minimizing iron solubilization. Kumari et al. [25] demonstrated that roasting at 850 °C for 6 h effectively converts metallic iron into Fe_2O_3, significantly suppressing its dissolution during acid leaching. Conversely, Gergoric et al. [30] applied a milder treatment at 400 °C for 1.5 h, which likely resulted in partial oxidation or simple demagnetization, limiting its effectiveness in reducing iron solubility. Ultimately, the complete disappearance of α-Fe and the rise of Fe_2O_3 and $NdFeO_3$ peaks after 6 h at 850 °C confirmed full oxidation.

This overall phase evolution also indicates that roasting not only passivates iron but also breaks the strong metallic and partially covalent bonding within the $Nd_2Fe_{14}B$ matrix, converting REEs into oxide environments that govern their subsequent leaching behavior.

From a chemical standpoint, thermal oxidation promotes both the passivation of iron and the breakdown of the Nd–Fe–B intermetallic phase into simpler oxide phases. The main oxidation reactions can be schematically expressed as:

$$4\,Fe + 3\,O_2 \rightarrow 2\,Fe_2O_3$$

$$2\,REE + 3\,O_2 \rightarrow 2\,REE_2O_3 \text{with REE} = \text{Nd, Pr, Dy}$$

$$Nd_2O_3 + Fe_2O_3 \rightarrow 2\,NdFeO_3$$

These reactions illustrate how roasting converts the metallic and partially covalent Nd–Fe–B matrix into iron oxides and rare-earth-containing oxide phases, thereby suppressing iron solubility while chemically activating REEs through structural oxidation. These structural changes are expected to influence subsequent leaching behavior, improving selectivity through the reduced solubility of oxidized iron phases in acidic media.

3.1.2. *Effect of roasting on the leaching treatment*

To evaluate the impact of thermal oxidation on selective leaching, HD powders roasted at 850 °C for 1, 2, and 6 h were subjected to leaching under conditions adapted from Gergoric [30]: 1 mol/L acetic acid, 400 rpm agitation, 23 ± 1 °C, S/L = 20 g/L, and a 24-h duration. The use of acetic acid under these conditions was intended to isolate the

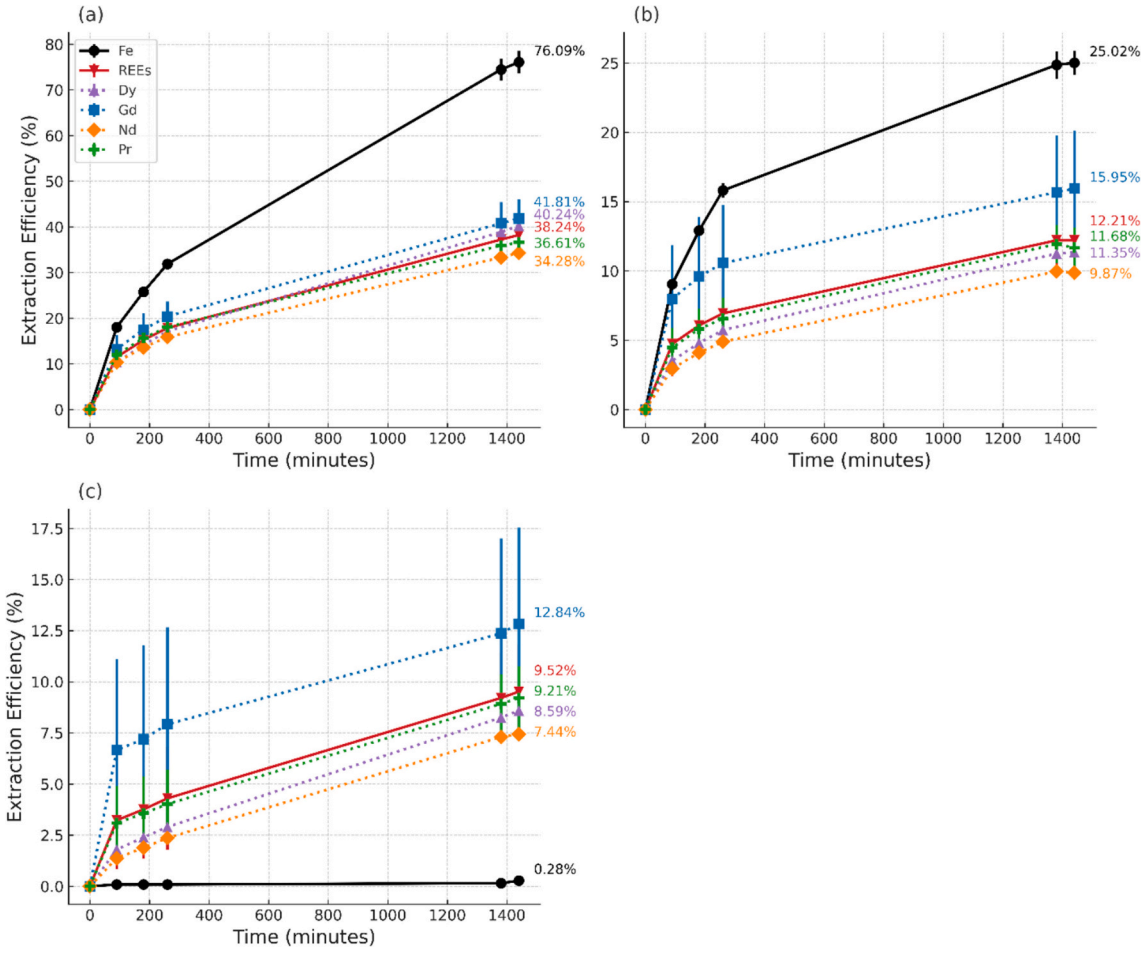

Fig. 4. Leaching efficiency by 1 mol/L acetic acid as a function of time after thermal pretreatment of the HD powder during (a) 1 h, (b) 2 h and (c) 6 h. (temperature = 23 °C; S/L = 20 g/L, 400 rpm).

effect of complete oxidative roasting on leaching behavior using a reference organic acid previously reported in the literature. The corresponding REEs and iron dissolution efficiencies are shown in Fig. 4 and are supported by XRD patterns before and after leaching (Figures SI-1–SI-3 in Supporting Information).

For the sample roasted for 1 h, the average dissolution efficiency of REEs is 38.2%, with individual solubilization efficiencies of 34.3% for Nd, 36.6% for Pr, 40.2% for Dy, and 41.8% for Gd. Iron dissolution is notably high at 76.1%. XRD analysis reveals the disappearance of the α-Fe peak after leaching, confirming significant iron removal, while other phase peaks remain unchanged. After 2 h of roasting, REEs leaching efficiency drops significantly to an average of 21.2%, and iron dissolution decreases to 25.0%. Although the α-Fe peak is again absent in the post-leaching XRD patterns, the overall phase composition remains stable, suggesting partial oxidation and reduced iron solubility. In the 6-h roasted sample, REEs dissolution efficiencies further declines to 9.5% on average (Nd: 7.4%, Pr: 9.2%, Dy: 8.6%, Gd: 12.8%), while iron solubility is reduced dramatically to 0.3%. The XRD pattern confirms complete oxidation, as indicated by the absence of α-Fe and the presence of Fe_2O_3 and $NdFeO_3$. Slight reductions in peak intensities across the patterns correlated with the modest leaching of REEs.

These results demonstrate a clear trend: increasing the roasting duration reduces iron dissolution, due to the formation of insoluble iron oxides such as Fe_2O_3 and $NdFeO_3$. However, this selectivity comes at the cost of reduced REE recovery. The 1-h treatment yielded the highest REE solubilization but failed to suppress iron dissolution, while the 6-h treatment achieved strong selectivity with minimal iron leaching but poor REE recovery. This trade-off highlights the challenge in ensuring both high selectivity and extraction efficiency. Comparatively, Gergoric [30] reported high REEs leaching under similar conditions, but applied a lower roasting temperature of 400 °C for 1.5 h, likely demagnetizing rather than oxidizing the material. This fundamental difference in thermal treatment likely explains the higher dissolution efficiencies for both REEs and iron in this study, which contrasts with the selective leaching observed in this work. The observed selectivity aligns with the findings of Reisdörfer [31] and Kumari [25], who emphasized the benefits of pre-roasting NdFeB magnets to enhance separation between REEs and iron. Although this pre-treatment hinders REE solubility under mild leaching conditions, it converts REEs into stable oxide or orthoferrite phases ($NdFeO_3$) whose high lattice stability kinetically limits proton-driven dissolution. However, this transformation simplifies downstream processing by eliminating the need for extensive purification, which is often reagent-intensive and environmentally burdensome.

In conclusion, roasting at 850 °C significantly improves iron selectivity during leaching but simultaneously limits REE recovery. This underscores the importance of developing leaching strategies tailored to oxidized magnet powders. Future investigations will focus on improving REE solubilization from 6-h roasted powders, aiming to maintain the low iron dissolution benefits of thermal pre-treatment while enhancing rare earth extraction through modifications in leaching chemistry or conditions.

3.2. Leaching

3.2.1. Effect of acid concentration and chloride ion addition

To evaluate whether acetic acid concentration and chloride ion addition could improve REEs extraction from roasted magnet powder while minimizing iron dissolution, leaching experiments were conducted during 24 h at 23 ± 1 °C with 400 rpm agitation and S/L = 20 g/L. Using acetic acid concentrations from 1 to 5 mol/L, REE leaching peaked at 24.5% with 3 mol/L, then declined at higher concentrations, while iron dissolution remained low (<0.25%). Addition of NaCl at 0.2 and 0.5 mol/L resulted in REEs leaching efficiencies of 15.0% and 16.0%, respectively, with iron dissolution under 0.2%. These results indicate that neither increasing the acid concentration nor adding chloride ions significantly enhanced REE extraction efficiency, confirming that acetic acid alone is insufficient for effective REE recovery under the tested conditions.

3.2.2. Influence of the nature of the acid

To investigate the influence of acid strength on the leaching efficiency of REEs from roasted HDD magnet powder, a series of leaching experiments were conducted using inorganic acids and organic of varying pK_a values. The aim was to evaluate the relationship between acid dissociation strength and REE solubilization while maintaining minimal iron dissolution. Organic acids are generally considered to be less environmentally impactful than inorganic acids, as they tend to exhibit lower impacts in categories when assessed through life cycle analysis. This is largely attributed to their biodegradability, lower energy requirements during synthesis, and reduced emissions during use and disposal. Therefore, in addition to assessing leaching efficiency, the potential environmental advantages of organic acids make them attractive alternatives for sustainable hydrometallurgical processes. However, it is important to consider their efficiencies to ensure complete recovery of metals [37]. All experiments involving organic acids were performed during 24 h at 23 ± 1 °C, with agitation set at 400 rpm, S/L = 20 g/L, and acid concentration of 1 mol/L.

The newly investigated leaching systems included citric acid (pK_{a1} = 3.1, pK_{a2} = 4.76, pK_{a3} = 6.4), trichloroacetic acid (TCA, pK_a = 0.67), methanesulfonic acid (MSA, pK_a = −1.9), and hydrochloric acid (pK_a = −6.3), whereas acetic acid (pK_a = 4.8) was investigated in the previous section. The variation of the extraction efficiency vs. leaching time for each new acids is reported in Fig. 5.

Citric acid, despite being triprotic, exhibited limited REE dissolution: 5.3% for Nd, 6.3% for Pr, 5.4% for Dy, and 5.7% for Gd, along with low iron dissolution (0.3%). For comparison, acetic acid exhibited similarly poor performance (Fig. 4c), with very limited REE dissolution (average 9.5%) and negligible iron solubility (0.3%) under the investigated conditions. TCA significantly improved leaching, achieving 29.2% for Nd, 33.2% for Pr, 28.9% for Dy, and 28.6% for Gd, with iron solubility remaining at 0.1%. MSA demonstrated the highest REE extraction among the organic acids with leaching efficiencies of 39.6% (Nd), 44.2% (Pr), 40.8% (Dy), and 41.9% (Gd), and iron dissolution of 0.3%.

Leaching with hydrochloric acid was evaluated under the following modified conditions adapted from Gergoric [30] and Kumari [25] (Fig. 5d): HCl concentration of 0.5 mol/L, increased S/L ratio of 100 g/L, and 500 rpm agitation. Despite the reduced acid concentration and higher solid loading, HCl achieved an average REE dissolution of 41.5% after 24 h. More specifically, 40.1% Nd, 40.3% Pr, 41.3% Dy, and 44.2% Gd were dissolved under these conditions after 24 h. These results are comparable to those of MSA, although iron dissolution was notably higher (leaching efficiency = 4.5%), which may necessitate expensive post-leaching purification steps due to the abundance of iron in the feedstock.

Overall, the data clearly demonstrate that lower pK_a values are associated with enhanced REE leaching efficiency, confirming that acid strength plays a pivotal role in the dissolution process. While citric acid and acetic acid exhibited limited performance, both TCA and MSA, along with HCl, substantially increased REE recovery while maintaining varying degrees of selectivity against iron. However, even with the strongest acids, the maximum REE dissolution remained around 40–44%, indicating that further optimization is necessary for industrial application.

The leaching curves in Fig. 5 suggest that equilibrium was not reached within 24 h for weaker acids, implying that extended treatment times or acid replenishment could further enhance extraction, particularly for citric acid and TCA. For MSA, the plateau in dissolution hints at acid depletion. Moreover, although HCl provides strong performance, its increased iron co-dissolution raises environmental and processing concerns. Enhancing temperature or optimizing acid concentration and S/L ratios may improve leaching without drastically increasing environmental burden.

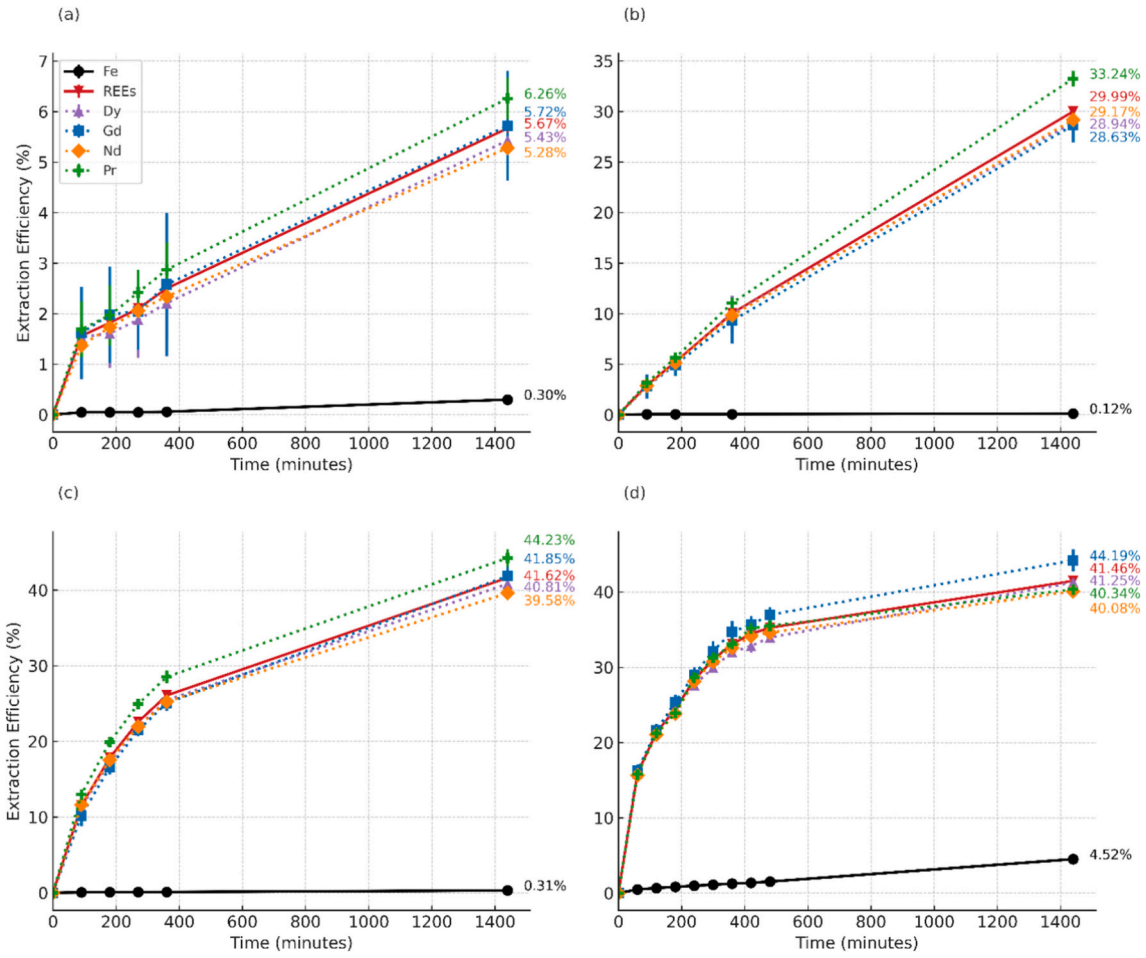

Fig. 5. Leaching efficiency of REEs and Fe by 1 mol/L (a) citric acid, (b) TCA, (c) MSA (temperature = 23 °C; S/L = 20 g/L, 400 rpm) and by 0.5 mol/L (d) HCl (temperature = 23 °C; S/L = 100 g/L, 500 rpm) as a function of leaching time after thermal pretreatment of the HD powder during 6 h.

Finally, the observed differences in solubility point to selective dissolution behavior, which could be further understood through the lens of Pearson's Hard and Soft Acids and Bases (HSAB) theory [38,39]. This framework can offer valuable mechanistic insights into the interactions between REEs, iron species, and the various acid media employed, guiding future strategies for selective and efficient REE recovery. REEs such as Nd, Pr, Dy, and Gd are classified as hard acids due to their high charge density and low polarizability. Iron, depending on its oxidation state, can be classified as either Fe^{3+} (hard acid), as in $FeNdO_3$, or Fe^{2+} (borderline acid), as found in Fe_3O_4. During roasting, iron is primarily oxidized to Fe^{3+}, stabilizing it in insoluble oxide phases.

The acids investigated in this study differ both in their intrinsic acidity and in the chemical nature of their conjugate bases, which together govern their leaching behavior. In the case of organic acids, metal dissolution may proceed through a combination of proton-driven attack and metal–ligand complexation. However, acetic and citric acids did not show efficient dissolution of REEs, indicating that ligand complexation alone is insufficient to destabilize rare earth oxide phases in the solid matrix. In contrast, the use of TCA and MSA leads to a gradual but still limited increase in REE dissolution. This behavior suggests that leaching is primarily controlled by proton activity rather than by the formation of stable metal–ligand complexes. Iron remains undissolved under all tested conditions, reflecting the high chemical stability of the ferric phase in the material.

These observations can be rationalized within the framework of the hard and soft acids and bases (HSAB) theory. Acetic acid (pKa = 4.8), citric acid ($pKa_1 = 3.1$, $pKa_2 = 4.76$, $pKa_3 = 6.4$), and trichloroacetic acid (pKa = 0.7) are organic acids whose conjugate bases (acetate, citrate, and trichloroacetate) behave as soft bases. Methanesulfonic acid (pKa = −1.9) is a stronger acid associated with a borderline base (methanesulfonate), whereas hydrochloric acid (HCl, pKa = −6.3) is a strong inorganic acid providing hard base chloride ions (Cl^-).

According to HSAB theory, hard acids preferentially interact with hard bases, and avoid forming stable complexes with soft bases. This explains the observed leaching behavior: citric acid and acetic acid resulted in poor REE dissolution and negligible iron solubility due to poor acid strength and a soft conjugate base. TCA moderately improved REE extraction (30%) while still maintaining low Fe dissolution (<0.2%) – a result of increased acidity and slightly stronger base strength. MSA, with stronger acidity and a borderline base, achieved the highest REE recoveries (42%), while keeping Fe dissolution minimal (<0.3%), thanks to both its acidity and better compatibility with hard metal centers. HCl also reached high REE dissolution (up to 44.2%), attributed to its very low pK_a value and the hard nature of Cl^-, which strongly favors complexation with REEs. However, Fe^{3+} was also partially solubilized (4.5%), due to its similar hard acid nature, reducing selectivity.

This can be explained since a small fraction of Fe that can be co-dissolved is found in compound along with the REEs. Consequently, when a moderate amount of REEs is extracted, iron dissolution remains naturally low. This explains why even in the most effective cases, REE dissolution reaches only 44%, while iron remains largely in the residue, except for the minor amount structurally associated with REE phases.

The general leaching reactions for REE and Fe oxides are:

$$M_2O_3(s) + 6\ CH_3COOH(aq) \rightarrow 2\ M(CH_3COO)_3(aq) + 3\ H_2O(aq)$$

$$M_2O_3(s) + 6\ CCl_3COOH(aq) \rightarrow 2\ M(CCl_3COO)_3(aq) + 3\ H_2O(aq)$$

$$M_2O_3(s) + 6\ CH_3SO_3H(aq) \rightarrow 2\ M(CH_3SO_3)_3(aq) + 3\ H_2O(aq)$$

$$M_2O_3(s) + 6\ HCl(aq) \rightarrow 2\ MCl_3(aq) + 3\ H_2O(aq)$$

To compare the intrinsic thermodynamic stability of Fe and REE oxide phases, the reactions were reduced to the simplified dissolution reaction:

$$M_2O_3(s) + 6H^+(aq) \rightarrow 2\ M^{3+}(aq) + 3H_2O(aq)$$

where M represents Fe or Nd. Standard Gibbs free energies of formation were taken from The NBS Tables of Chemical Thermodynamic Properties (JPCRD, Vol. 11, Suppl. 2). [40] The values used (kJ.mol^{-1}) were: $Fe^{3+} = -4.7$, $Fe_2O_3 = -742.4$, $Nd^{3+} = -671.6$, $Nd_2O_3 = -1720.8$, and $H_2O = -237.129$. For iron oxide dissolution, the standard Gibbs free energy change is equal to $\Delta G^\circ = +21.6$ kJ.mol^{-1}, indicating that Fe_2O_3 remains thermodynamically resistant to proton attack under standard conditions. For neodymium oxide, the standard Gibbs free energy change is $\Delta G^\circ = -333.8$ kJ.mol^{-1}, demonstrating a thermodynamic driving force for REE dissolution.

This thermodynamic contrast directly explains the observed selectivity after roasting. Iron is effectively passivated as Fe_2O_3, whose dissolution remains unfavorable even under acidic conditions, whereas REE oxides exhibit an intrinsic tendency toward dissolution. The nature of the acid system modulates the effective Gibbs free energy of REE leaching through proton activity and speciation in solution, leading to progressively higher leaching efficiencies from citric acid to TCA, MSA and HCl. In contrast, the dissolution of Fe_2O_3 remains thermodynamically constrained across all systems, and the small amount of iron detected in solution is mainly associated with the co-dissolution of REE-bearing phases rather than bulk iron oxide.

3.2.3. Effect of the temperature

In order to reach quantitative dissolution of REEs, temperature is a significant factor that influences acid leaching through multiple interrelated mechanisms. Elevated temperatures increase molecular kinetic energy, accelerating reaction rates by surpassing activation energy barriers. They also enhance solid solubility and ion diffusion, improving mass transfer between phases – crucial for effective leaching. Additionally, higher temperatures may increase acid dissociation, further promoting metal extraction. However, they can also induce side reactions or thermal decomposition, potentially reducing leaching efficiency or introducing impurities. To investigate the thermal enhancement of leaching using TCA, MSA, and HCl, experiments were conducted at 93 °C. Experimental conditions for TCA and MSA followed Gergoric's protocol (1 mol/L acid, 400 rpm, S/L = 20 g/L ratio, 24 h) [30], while HCl experiments employed Kumari's conditions (0.5 mol/L acid, 500 rpm, S/L = 100 g/L) [25].

Leaching results are presented in Fig. 6 for (a) TCA, (b) MSA, and (c) HCl. Heating prior to leaching enhanced the dissolution of REEs across all acids, though performance varied. With TCA, leaching efficiencies were 33.7% for Nd, 33.4% for Pr, 50.5% for Gd, and 55.3% for Dy, while iron remained largely insoluble (0.3%). Although elevated temperature improved REE recovery, efficiency declined after 180 min, likely due to acid degradation and subsequent REE precipitation. MSA yielded significantly higher dissolution rates, with an average REE recovery of 87.1%. Individual leaching efficiencies reached 82.2% for Nd, 86.1% for Pr, 86.9% for Gd, and 93.3% for Dy, indicating near-complete extraction. However, iron solubility also increased to 9.7%, suggesting a need for further purification steps. HCl demonstrated the highest efficiency, achieving complete REE dissolution within 9 h – substantially faster than the 24-h leaching required for TCA and MSA. Iron dissolution remained minimal at 0.07%. These results are especially noteworthy given the lower acid concentration and higher S/L ratio used, underscoring the effectiveness of thermal enhancement. Overall, while TCA

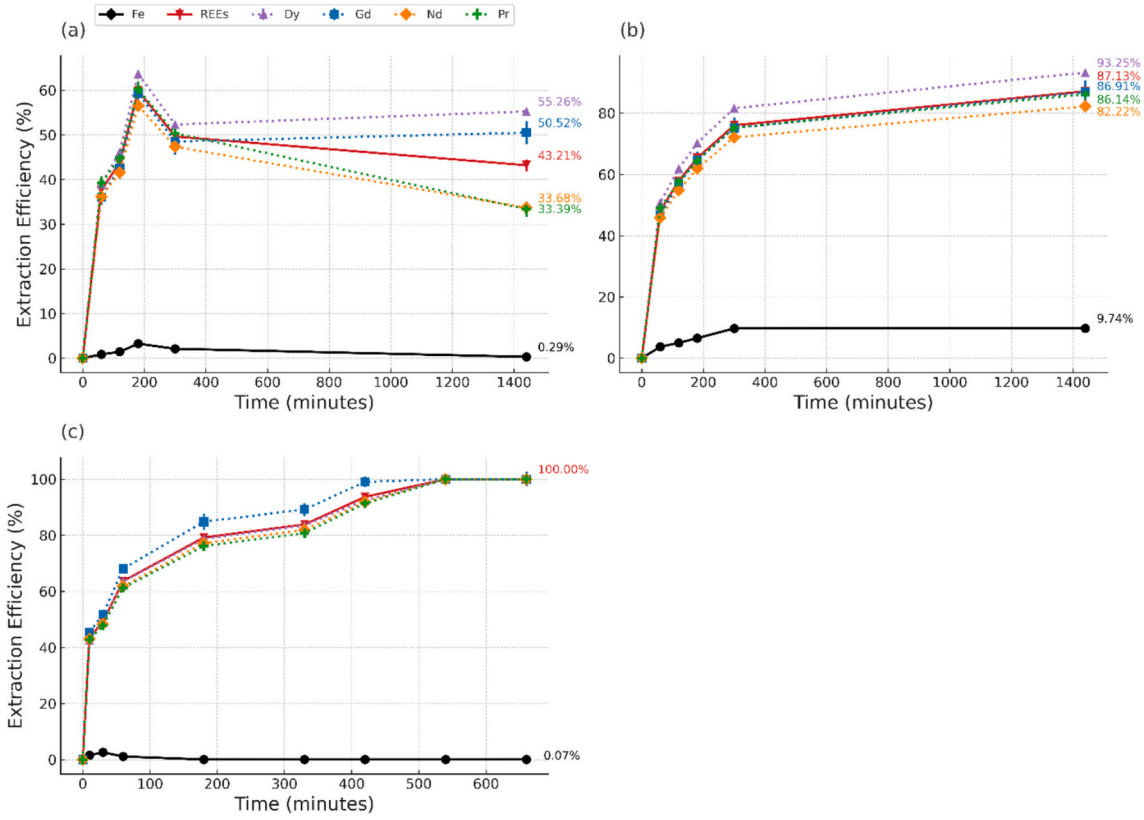

Fig. 6. Leaching efficiency of REEs and Fe at 93 °C by 1 mol/L of (a) TCA and (b) MSA, and (c) 0.5 mol/L of HCl as a function of leaching time after thermal pretreatment of the HD powder during 6 h. (TCA/MSA: S/L = 20 g/L, 400 rpm – HCl: S/L = 100 g/L, 500 rpm).

and MSA showed improved REE leaching with heating, HCl achieved complete dissolution in less time with minimal iron contamination, indicating its superior potential for industrial applications.

At elevated temperature (93 °C), the thermodynamic driving force for oxide dissolution was evaluated using the Gibbs free energy relation $\Delta G = \Delta H - T\Delta S$ applied to the simplified reaction:

$$M_2O_3(s) + 6H^+(aq) \rightarrow 2\,M^{3+}(aq) + 3H_2O(l)$$

By using thermodynamic data [40], Fe_2O_3 dissolution yields ΔG° (298 K) $\approx +21.6$ kJ.mol^{-1} and ΔG°(366 K) $= +56.2$ kJ.mol^{-1}, confirming that iron oxide remains thermodynamically resistant to acid attack at elevated temperature. In contrast, Nd_2O_3 exhibits ΔG°(298 K) $= -334$ kJ.mol^{-1} and ΔG°(366 K) $= -309$ kJ.mol^{-1}, indicating that REE oxides remain prone to dissolution at elevated temperature. In addition, no leaching plateau was previously reached at 23 °C within the investigated contact time, indicating that dissolution is kinetically limited at room temperature. The marked increase in REE recovery observed at 93 °C therefore results from both a strong thermodynamic driving force and a pronounced acceleration of dissolution kinetics due to higher temperature, while iron remains effectively passivated.

Leaching experiments using MSA and HCl also revealed distinct dissolution behaviors for non-REE elements, as shown in Fig. 7. In the MSA system (a), several elements exhibited substantial solubilization. Boron showed the highest non-REE dissolution at 77.1%, closely paralleling the behavior of REEs. Copper and cobalt were also significantly leached, with efficiencies of 64.9% and 61.8%, respectively, consistent with trends observed in prior roasting experiments. Aluminum and niobium displayed the same leaching efficiencies of 52.3%. In contrast, gallium remained largely insoluble, with only 6.2% dissolution. Under HCl leaching (b), boron again exhibited complete dissolution after 660 min of treatment and 90.7% after 540 min. However, aluminum dissolution was substantially reduced (25.9%), and gallium, cobalt, and copper were only minimally solubilized, with respective efficiencies of 5.3%, 3.1%, and 1.4%. Overall, MSA facilitated greater co-leaching of elements such as B, Cu, Co, and Nb compared to HCl, suggesting its potential for multi-element valorization. Notably, boron achieved high recovery in both systems, indicating potential for co-extraction alongside REEs. In contrast, HCl's selectivity – keeping Ga, Cu, and Co largely insoluble – may be advantageous for processes prioritizing REE purity. Heating improved dissolution kinetics in both acids, consistent with the Pearson HSAB theory, by enhancing interactions between acid species and metal ions. The higher dissolution of Cu, Co, and Nb in MSA reflects the softer and borderline nature of methane sulfonate, which forms more stable complexes with these metals than chloride ions do. Additionally, MSA experiments involved smaller powder masses exposed to longer treatment times and greater acid availability per unit mass, possibly explaining the higher aluminum recovery in MSA. Conversely, aluminum remained less soluble in HCl, likely due to the persistence of refractory aluminum oxides.

Overall, temperature was identified as the decisive parameter enabling efficient leaching of rare-earth elements from fully oxidized NdFeB magnet powder while preserving iron selectivity. At room temperature, REE dissolution remained kinetically limited regardless of acid strength, even for strong acids such as MSA and HCl. Increasing the temperature to 93 °C resulted in a marked acceleration of leaching kinetics and, more importantly, enabled near-complete or quantitative dissolution of REEs within industrially relevant timescales.

Thermodynamic analysis confirmed that this behavior is intrinsic to the oxide phases generated during roasting. While REE oxides and orthoferrites exhibit a strong thermodynamic driving force for dissolution, iron remains stabilized as Fe_2O_3, whose dissolution is unfavorable even at elevated temperature. As a result, heating enhances REE selectively dissolution without compromising iron passivation, validating roasting as an effective phase-engineering step rather than a simple pretreatment.

Among the acids investigated, temperature amplification revealed distinct process windows. TCA showed moderate improvement but remained limited by acid stability and partial precipitation effects. MSA enabled high REE recoveries but at the expense of increased co-dissolution of iron and transition metals. In contrast, hydrochloric acid combined elevated temperature with high solid loading and low acid concentration to achieve complete REE dissolution within 9 h, while maintaining minimal iron solubilization.

These results demonstrate that temperature acts as a key lever to overcome kinetic barriers imposed by oxidative roasting, allowing selective and efficient REE recovery under conditions compatible with industrial implementation. When coupled with controlled phase transformation during roasting, thermal enhancement enables a robust leaching strategy that maximizes REE recovery while minimizing downstream purification requirements.

3.2.4. *Organic acids vs. HCl*

The comparison between organic and inorganic acids is often framed in terms of intrinsic environmental impact, with organic acids commonly perceived as more sustainable alternatives. However, once oxidative roasting is applied as a phase-engineering step, this comparison must be reconsidered at the process level rather than at the level of isolated reagents.

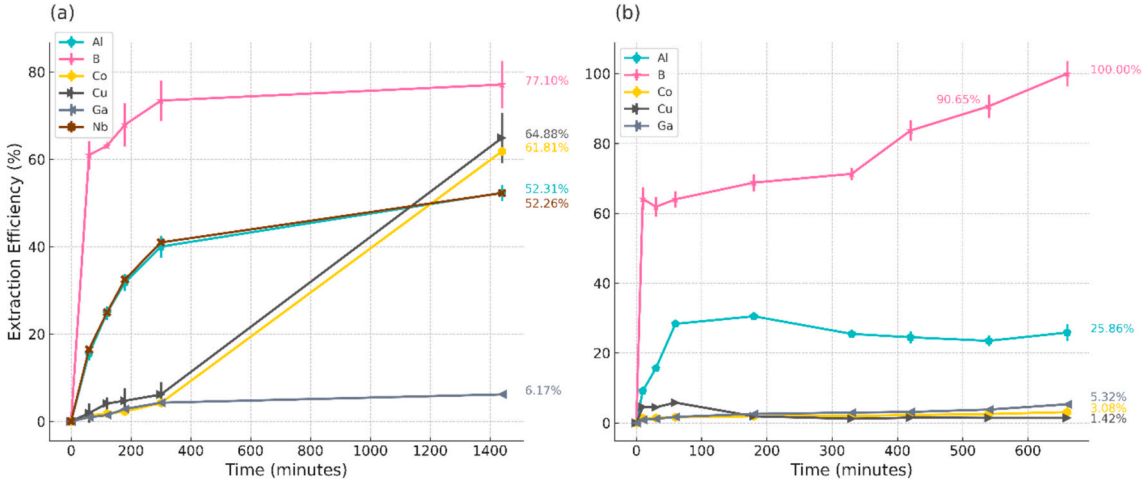

Fig. 7. Leaching efficiency of other elements (Al, B, Co, Cu, Ga and Nb) by (a) 1 mol/L MSA and (b) 0.5 mol/L HCl as a function of leaching time after thermal pretreatment of the HD powder during 6 h 93 °C. (MSA: S/L = 20 g/L, 400 rpm – HCl: S/L = 100 g/L, 500 rpm).

Under mild leaching conditions, organic acids such as citric acid, TCA, and MSA exhibited limited to moderate REE dissolution, even when heating was applied. Although elevated temperature significantly enhanced REE recovery with MSA, this improvement was systematically accompanied by increased co-dissolution of iron and transition metals. Such behavior directly increases the complexity of downstream separation, requiring additional solvent extraction stages, higher reagent consumption, and ultimately a larger environmental footprint.

In contrast, HCl demonstrated a fundamentally different performance window. Despite being used at lower concentration (0.5 mol/L) and under high solid loading (100 g/L), HCl enabled complete REE dissolution within 9 h at 93 °C while maintaining iron solubilization at negligible levels (0.07%). This combination of fast kinetics, high selectivity, and high solid throughput directly translates into reduced reactor volumes, shorter residence times, and simplified post-leaching processing.

From an environmental perspective, life cycle assessments reported by Kappenthuler et al. [41] for MSA and Modahl et Brekke [42] for HCl, based on the same functional unit (1000 kg of acid produced), indicate that the global warming potential associated with MSA production can significantly exceed that of HCl, particularly for conventional synthesis routes. When integrated at the process scale, the higher acid consumption, longer leaching times, and increased downstream purification requirements associated with MSA further amplify this difference. These results highlight that reagent selection must be evaluated in relation to the entire hydrometallurgical flowsheet rather than based on perceived intrinsic "greenness".

Under the favorable conditions identified in this study, leaching with HCl produced a pregnant leach solution characterized by high REE concentrations and limited impurity levels. The composition of this solution is reported in Table 2. Neodymium reached 18.51 g/L, accompanied by 2.71 g/L Dy, 1.31 g/L Pr, and 1.20 g/L Gd, while iron was reduced to only 0.24 g/L despite its initial abundance in the magnet feed. The limited concentrations of aluminum (0.22 g/L) and boron (0.67 g/L) further confirm the high selectivity achieved through the combined roasting–HCl leaching strategy.

These results demonstrate that, when oxidative pretreatment is used to control solid-phase chemistry, hydrochloric acid provides the most robust and process-compatible leaching medium. Its use enables high REE recovery under intensified yet selective conditions, while minimizing downstream separation burdens and overall environmental impact.

3.3. Leachate post-processing

The composition of the leachate given in Table 2, characterized by high REEs dissolution and minimal iron solubilization, highlights the potential for implementing solvent extraction strategies. However, the complexity of the leachate including numerous co-elements along the REEs require an accurate strategy to limit the environmental impacts and the use of high quantity of solvents during the post-leaching processing steps. Considering the high LREEs content (around 20 g/L) and the medium HREEs content, a reasonable strategy would be to isolate as much as possible the LREEs from the HREEs and the co-leached elements.

The separation of REEs from acid leachates remains a major challenge due to the chemical similarity of lanthanides and the frequent presence of co-dissolved metals. Among solvent extraction reagents, acidic organophosphorus extractants such as di-(2-ethylhexyl)-phosphoric acid (D2EHPA) are widely recognized for their high affinity toward trivalent rare earth ions [43]. D2EHPA operates through a cation-exchange mechanism, in which metal extraction is driven by the formation of neutral metal-extractant complexes and the simultaneous release of protons to the aqueous phase. The extraction strength of D2EHPA is known to increase along the lanthanide series as the ionic radius decreases, reflecting the increasing charge density and decreasing hydration energy of HREEs [44]. Consequently, D2EHPA exhibits an intrinsic preference for HREEs over LREEs making their separation possible during the extraction step and facilitated during stripping. [45]

However, the application of D2EHPA alone to highly acidic leachates is often associated with practical and selectivity-related limitations, including reduced extraction efficiency at low pH, co-extraction of competing trivalent metals such as Fe(III), and high organic phase viscosity at elevated metal loadings. [43,45] To address these issues and to explore potential synergistic effects, tri-n-butyl phosphate (TBP) was selected as a co-extractant and phase modifier in combination with D2EHPA.

Very few studies investigated the synergistic effect of TBP and D2EHPA to extract REEs. From nitrate acidic leachate, it has been reported that the mixture can enhance HREEs extraction and increase separation factor with the LREEs [46,47]. When combining it with D2EHPA, TBP can stabilize metal-extractant complexes in the organic phase through solvation effects, leading to enhanced extraction of strongly interacting species under more acidic conditions. Any apparent synergy between D2EHPA and TBP under chloride conditions is expected to primarily affect HREEs through enhanced stabilization of D2EHPA–metal complexes, with a limited impact on LREE extraction at similar acidity.

Indeed, TBP is a neutral solvating extractant that does not exhibit significant affinity to trivalent rare earth ions under acidic chloride conditions, owing to the strong hydration of Ln^{3+} ions and their limited tendency to form extractable anionic complexes [45,48,49]. This characteristic makes TBP inert toward REEs, thereby preserving the inherent selectivity of D2EHPA over HREEs. At the same time, TBP is well known to extract non-REE metals that form stable neutral or anionic chloro-complexes, including Fe(III), [50,51] Ga(III) [52] and other high valence elements while it does not affect bore [53] or aluminum and cobalt [54]. For this reason, TBP has been extensively employed in hydrometallurgical flowsheets as a selective scavenger of co-leached metals from acidic solutions, while leaving REEs in the aqueous phase. Beyond its intrinsic extraction selectivity, TBP exhibits favorable physical properties, including low viscosity, good chemical stability, and rapid phase disengagement, which can improve mass transfer and phase separation during liquid–liquid extraction. The presence of TBP may therefore alleviate some of the operational drawbacks associated with the use of acidic extractants alone, particularly in systems involving complex leachates and high metal concentrations [55,56].

Based on these considerations, the working hypothesis was that D2EHPA would preferentially extract HREEs while LREEs would remain largely in the aqueous phase. TBP was expected to contribute to the removal of non-REE impurity metals and to enhance the stability and efficiency of the extraction system without promoting LREE- co-extraction. For this purpose, the extraction efficiency of the elements was evaluated using the leachate as the aqueous phase and a synergistic mixture of D2EHPA and TBP diluted in kerosene as organic phase (molar ratio = 1, O/A = 1). The solvent extraction test was performed to demonstrate feasibility and was not intended to represent an optimized separation flowsheet.

During the process, pH adjustment was not possible due to third-phase formation. Nevertheless, extraction without pH control showed that most Nd remained in the aqueous phase, while the other metals were successfully extracted. The results of this test are presented in

Table 2
Composition of the pregnant liquor solution obtained by dissolving roasted HD powder (HCl concentration = 0.5 mol/L, leaching temperature = 93 °C, roasting temperature = 850 °C for 6-h; S/L = 100 g/L, 500 rpm).

Elements	Nd	Dy	Pr	Gd	B	Al
	18.51	2.71	1.31	1.20	0.67	0.22
Concentration g/L	Fe	Nb	Co	Ge	Cu	Ga
	0.24	0.037	0.031	0.013	0.008	0.001

Table 3
Extraction efficiency and composition of raffinate and the organic phase after liquid-liquid extraction using synergistic mixture of D2EHPA and TBP diluted in kerosene (molar ratio = 1, O/A = 1, shaking time = 30 min, temperature of shaking = 25 °C, pH at equilibrium = 0.605).

Element	Nd	Pr	Dy	Gd	Al	B	Co	Fe	Nb
Extraction Efficiency (%)	9.06	6.63	96.88	69.13	3.85	0.00	30.07	78.07	7.06
Concentration of the raffinate after extraction (g/L)	16.83	1.22	0.08	0.37	0.21	0.67	0.02	0.05	0.03
Composition of the organic phase (g/L)	1.68	0.09	2.63	0.83	0.01	0.0	0.01	0.2	0.0

Table 3. Efficient extraction of Dy and Gd was achieved while minimizing Nd losses. The synergistic mixture exhibited high extraction efficiencies for heavy REEs, reaching 96.88% for Dy and 69.13% for Gd, whereas extraction efficiencies for light REEs were significantly lower (9.06% for Nd and 6.63% for Pr). This system was shown to selectively enhance the extraction of heavy rare earths over light ones, due to the formation of more stable complexes and the lower affinity of the extractant for light REEs. [46,57,58]

The cation-exchange extraction occurring with D2EHPA can be expressed as:

$$Ln^{3+}_{(aq)} + 3(HR)_{2(org)} \leftrightarrow LnR_3.(HR)_{3(org)} + 3H^{+}_{(aq)}$$

Where $(HR)_2$ represents the hydrogen-bonded dimer of D2EHPA and (Ln^{3+}) the trivalent rare earth ions.

Concerning the extraction of the co-leached metals, 78.07% of Fe was extracted along with Co at 30.07%, Nb at 7.06% and Al at 3.85% while bore was not extracted by the mixture. Iron showed high extraction efficiency, which is consistent with the well-known strong affinity of Fe(III) for acidic organophosphorus extractants and TBP [45,50,51,59,60]. The cation-exchange reaction can also contribute to Fe^{3+} extraction, explaining its high efficiency. However, it should be noted that, even with elevated iron extraction, Fe was largely suppressed upstream by oxidative roasting and remains negligible relative to the rare-earth loading. Aluminum, boron, and niobium were either not extracted or showed very low extraction efficiency, as expected. Cobalt was slightly extracted, likely due to a weak but non-negligible cation-exchange interaction between Co(II) and D2EHPA under acidic conditions.

In contrast to D2EHPA, TBP form stable chloro-complexes by solvating neutral or anionic metal complexes with other metals such as Fe (III), Nb(V) and Ge(IV). This extraction can be represented by the following general reactions:

For anionic complexes:

$$MCl^{m-}_{n\ (aq)} + xTBP_{(org)} \leftrightarrow TBP_x.MCl_{n\ (org)}$$

and for neutral complexes:

$$MCl^{0}_{n\ (aq)} + xTBP_{(org)} \leftrightarrow TBP_x.MCl_{n\ (org)}$$

where (MCl) represents the metallic chloride ion.

Such solvation reactions are strongly dependent on chloride concentration and acidity but are largely independent on proton exchange equilibria. Because trivalent rare earth ions remain strongly hydrated and do not form extractable chloro-complexes under comparable conditions, their extraction by TBP alone is negligible.

This preliminary approach proved effective separation between HREES and LREEs as a first step for leaching post-processing. However, further optimization of the extraction step through a parametric study and multi-stage operation can achieve better loaded output streams and enhanced selectivity.

3.4. Flowsheet

Following liquid–liquid extraction using D2EHPA-TBP with acidic solutions, efficient recovery of LREEs and HREEs from the organic phase is possible in a two-step selective stripping. Previous studies showed that selective stripping between light and heavy REEs can be achieved by adjusting the acidity and the operating conditions of the stripping stage by using various mineral acids [61–63]. At low acid strengths, diluted mineral acids preferentially release LREEs such as Nd^{3+} and Pr^{3+}, whose metal–phosphoric complexes dissociate more easily under mild proton activity, while Dy^{3+} and Gd^{3+} remain strongly retained in the organic phase [63]. When the acidity is increased, HREEs become progressively strippable, making it possible to recover them in a second stage once the LREEs have been removed [62]. This behavior is consistent with the general trend that heavier lanthanides possess smaller ionic radii and form more stable complexes with phosphate, requiring higher proton concentrations to induce back-extraction [59,64,65].

Subsequent process such as oxalate precipitation can serve as a downstream recovery step for the raffinate and the two acidic strip liquors obtained after selective separation. LREEs can be efficiently precipitated from acidic solutions using oxalate, as demonstrated for magnet leachates where high selectivity over elements like Ni, Co, Al and B was achieved under mildly acidic conditions [66,67]. The precipitation was performed at room temperature with a molar excess of oxalate ($C_2O_4^{2-}$/REE > 3:2) and under acidic conditions (pH = 1.5) ensuring 95% of REEs recovery.

Broader studies on rare-earth precipitation have shown that the oxalate route is applicable not only to LREEs but also to HREEs, since Dy^{3+} and Gd^{3+} form very sparingly soluble oxalates [68,69]. Studies has shown that Dy^{3+} and Gd^{3+} exhibit distinct solubility behaviors depending on the nature of the precipitant and pH, enabling selective or sequential precipitation under controlled conditions [68]. Consistent with this, the U.S. Department of Energy has reported that HREEs such as Dy and Gd can also be selectively recovered from mixed streams using oxalate precipitation [70]. Although HREEs generally require tighter control of acidity and oxalate dosage because of their stronger hydration and solution complexation [69], their recovery by oxalate precipitation remains fully feasible. As a complementary approach, precipitation therefore offers a feasible and tunable method for recovering REEs after selective stripping. The resulting REE oxalate, $(REE_2(C_2O_4)_3).nH_2O$, can be calcined to form oxides and further reduced for magnet production [71].

Looking at co-elements such as Al and B, their recovery may offer both environmental and economic benefits. Although aluminum may co-precipitate with REEs during the oxalate precipitation step, its concentration in the raffinate remains much lower than that of Nd and Pr, which limits its overall impact on REEs precipitation. In addition, a dedicated downstream removal step remains feasible. Zhu et al. [72] demonstrated an effective method to selectively recover Al from chloride-rich media by regulated hydrolysis under electrochemical control. In their study, Al was precipitated as aluminum oxyhydroxide (AlOOH) with 88.35% removal and less than 6% REE loss providing a reagent-free and selective strategy fully compatible with hydrochloric media. For boron, Lin et al. [73] proposed a chemical oxo-precipitation approach, involving the addition of hydrogen peroxide and barium hydroxide to promote borate formation and precipitation. This process, performed at room temperature, enabled boron removal efficiencies above 99%, and is applicable even in highly acidic environments.

Therefore, Fig. 8 summarizes a global process implementing roasting, leaching, solvent extraction with D2EHPA-TBP mixture and the overall post-extraction route previously discussed for the recovery of REEs from HD magnet powder.

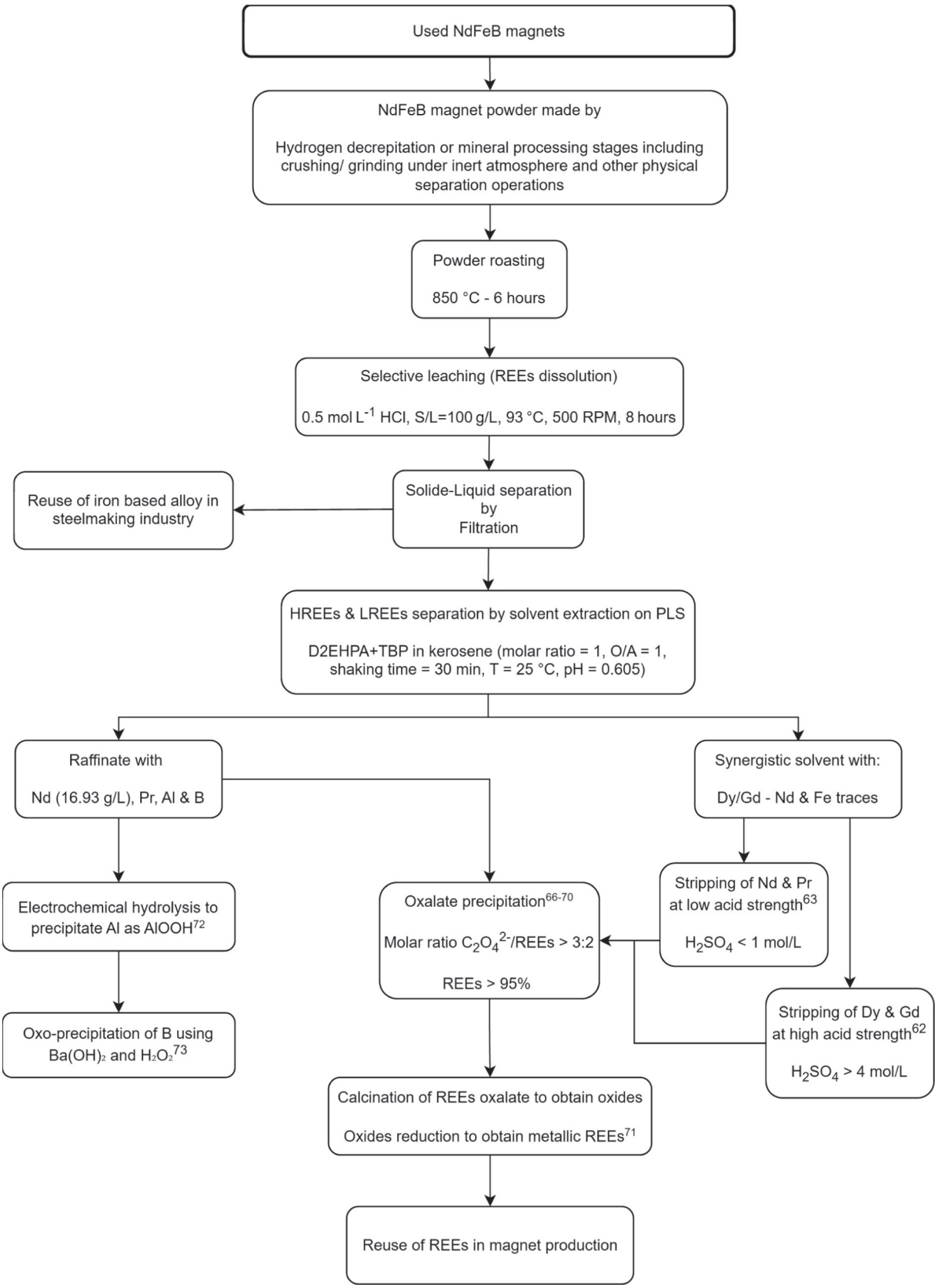

Fig. 8. Hydrometallurgical Flowsheet for Selective REE Recovery and Co-element Valorization from Roasted Powder of End-of-Life HDD Magnets.

The advantages of the proposed route arise from the deliberate control of the physicochemical state of the magnet powder prior to leaching, whereby oxidative roasting is used to govern the dissolution behavior of both rare-earth and non-rare-earth elements. By stabilizing iron in poorly soluble oxide phases prior to contact with the leaching solution, selective dissolution conditions are established that are governed primarily by solid-state chemistry rather than by fine-tuning of the leaching parameters.

This upstream control enables leaching conditions that combine high rare-earth recovery with limited impurity transfer to the solution. As a result, the pregnant leach solution exhibits elevated rare-earth concentrations and low levels of interfering elements, which inherently favors efficient downstream separation by solvent extraction or selective precipitation. The reduced impurity load simplifies process design and limits the need for additional purification or corrective treatment steps.

An additional benefit of this approach is the early integration of impurity management within the flowsheet. The dissolution behavior of accompanying elements such as iron, aluminum, boron, and transition metals can be anticipated and controlled at the leaching stage, thereby avoiding their uncontrolled accumulation in downstream circuits. This contributes to a more compact and robust process layout, with lower reagent consumption and reduced operational complexity.

From an environmental perspective, the proposed route should be evaluated at the scale of the overall process rather than through isolated unit operations. While oxidative roasting involves an energy input, it enables leaching under conditions combining high solid-to-liquid ratios, reduced acid concentration, shorter residence times, and simplified downstream separation. The ability to process larger amounts of material per batch, together with lower chemical demand and limited purification requirements, leads to a reduced cumulative environmental burden compared with routes based on extended leaching or chemically intensive treatment schemes. This process-level assessment is consistent with recent analyses of NdFeB magnet recycling, which identify selective pretreatment, minimized reagent consumption, and streamlined downstream operations as key drivers of sustainability [74,75].

Finally, the proposed methodology supports sustainability by promoting resource efficiency and process flexibility. The generation of a concentrated and selectively purified rare-earth stream, combined with the possibility of valorizing co-elements through dedicated recovery routes, aligns with circular-economy principles. The integration of phase transformation, selective leaching, and compatibility with established separation technologies provides a scalable framework for the recycling of end-of-life NdFeB magnets under industrially relevant conditions.

4. Conclusion

This study investigated the hydrometallurgical recycling of NdFeB magnets derived from end-of-life hard disk drives, with a specific focus on understanding and controlling the dissolution behavior of both rare-earth elements and accompanying non-REE metals. The primary objective was not only to maximize REE recovery, but also to establish selective leaching conditions that limit iron solubilization and enable efficient downstream processing under industrially relevant constraints.

Oxidative roasting of hydrogen-decrepitated magnet powder at 850 °C was demonstrated to be a critical phase-engineering step. This treatment converts metallic iron into thermodynamically stable oxide phases while transforming the Nd–Fe–B matrix into rare-earth-bearing oxides and orthoferrites. As a result, iron dissolution is strongly suppressed during leaching, shifting the selectivity control from solution chemistry to solid-state chemistry. This upstream control fundamentally governs the leaching behavior and reduces reliance on complex downstream purification strategies.

Under these conditions, leaching at room temperature remained kinetically limited, regardless of acid type. Organic acids, although often considered for their perceived environmental benefits, did not provide a viable pathway toward complete REE recovery once full oxidation was achieved. Methanesulfonic acid enabled high REE recoveries only at elevated temperature, but at the expense of increased co-dissolution of iron and transition metals.

In contrast, hydrochloric acid emerged as the most robust leaching medium when combined with oxidative roasting and thermal activation. Complete dissolution of REEs was achieved at 93 °C using a low acid concentration (0.5 mol/L) and a high solid-to-liquid ratio (100 g/L), while iron solubilization remained negligible. These conditions produced a pregnant leach solution with high REE concentrations (e.g., 18.51 g/L Nd) and limited impurity levels, providing a chemically favorable feed for subsequent separation steps.

Preliminary solvent extraction experiments using a synergistic mixture of D2EHPA and TBP confirmed the suitability of the leachate for downstream processing. This system enabled preferential extraction of HREEs (Dy, Gd) while retaining most of the neodymium in the aqueous phase, illustrating a viable pathway for selective separation without extensive pH adjustment or complex reagent schemes. In addition, the controlled dissolution behavior of co-elements such as Al and B opens opportunities for their targeted removal or valorization using established precipitation or electrochemical techniques.

From a process and sustainability perspective, these results highlight that reagent selection must be evaluated at the scale of the entire flowsheet. Although oxidative roasting involves an energy input, it enables intensified leaching conditions combining high throughput, reduced acid consumption, shorter residence times, and simplified downstream processing. When considered holistically, this strategy offers a favorable balance between performance, selectivity, and environmental impact.

Overall, this work demonstrates that combining oxidative pretreatment with thermally enhanced hydrochloric acid leaching provides a selective and process-viable route for rare-earth recovery from end-of-life NdFeB magnets. By explicitly addressing the behavior of both REEs and co-extracted elements, the proposed approach contributes to the development of robust hydrometallurgical flowsheets aligned with circular-economy principles and the sustainable supply of critical raw materials.

CRediT authorship contribution statement

Nicolas Stankovic: Writing – original draft, Visualization, Investigation, Formal analysis. **Jérôme Marin:** Investigation, Formal analysis. **Julien Jourdan:** Formal analysis. **Thibault Quatravaux:** Writing – review & editing, Supervision, Formal analysis, Conceptualization. **Alexandre Chagnes:** Writing – review & editing, Writing – original draft, Supervision, Project administration, Funding acquisition, Formal analysis, Conceptualization.

Declaration of competing interest

The authors declare the following financial interests/personal relationships which may be considered as potential competing interests: Alexandre Chagnes reports financial support was provided by University of Lorraine. Alexandre Chagnes reports a relationship with University of Lorraine that includes: employment. If there are other authors, they declare that they have no known competing financial interests or personal relationships that could have appeared to influence the work reported in this paper.

Acknowledgements

The author would like to acknowledge the Lorraine University of Excellence, the LabEx RESSOURCES21 and the LabEx DAMAS for their financial supports. The author expresses his gratitude to Sophie Rivoirard from MagREEsources start-up for furnishing the decrepitated magnet powder and for her support and the enriching discussions.

Appendix A. Supplementary data

Supplementary data to this article can be found online at https://doi.org/10.1016/j.cej.2026.174024.

Data availability

Data will be made available on request.

References

[1] European Commission, Joint Research Centre, P. Alves Dias, S. Bobba, S. Carrara, B. Plazzotta, The Role of Rare Earth Elements in Wind Energy and Electric Mobility – An Analysis of Future Supply/Demand Balances, Publications Office of the European Union, 2020, https://doi.org/10.2760/303258.

[2] Dolf Gielen, Martina Lyons, Critical Materials for the Energy Transition: Rare Earth Elements, **2022**.

[3] J.H. Rademaker, R. Kleijn, Y. Yang, Recycling as a strategy against rare earth element criticality: a systemic evaluation of the potential yield of NdFeB magnet recycling, Environ. Sci. Technol. 47 (18) (2013) 10129–10136, https://doi.org/10.1021/es305007w.

[4] R. Skomski, Permanent magnets: history, current research, and outlook, in: a. Zhukov (Ed.), Novel Functional Magnetic Materials 231, Springer Series in Materials Science; Springer International Publishing, Cham, 2016, pp. 359–395, https://doi.org/10.1007/978-3-319-26106-5_9.

[5] S. Rivoirard, J.G. Noudem, P. de Rango, D. Fruchart, S. Liesert, J.L. Soubeyroux, Anisotropic and Coercive NdFeB Powder for Bonded Magnets. *Proceedings of the 16th Int. Workshop on Rare-Earth Magnets and Their Applications*, 2000.

[6] R. Nakayama, T. Takeshita, Nd2Fe14B anisotropic magnet powders produced by the HDDR process, J. Alloys Compd. 193 (1–2) (1993) 259–261, https://doi.org/10.1016/0925-8388(93)90364-S.

[7] H. Sepehri-Amin, W.F. Li, T. Ohkubo, T. Nishiuchi, S. Hirosawa, K. Hono, Effect of Ga addition on the microstructure and magnetic properties of hydrogenation–disproportionation–desorption–recombination processed Nd–Fe–B powder, Acta Mater. 58 (4) (2010) 1309–1316, https://doi.org/10.1016/j.actamat.2009.10.035.

[8] S. Sugimoto, Current status and recent topics of rare-earth permanent magnets, J. Phys. D. Appl. Phys. 44 (6) (2011) 064001, https://doi.org/10.1088/0022-3727/44/6/064001.

[9] M. Nakamura, M. Matsuura, N. Tezuka, S. Sugimoto, Y. Une, H. Kubo, M. Sagawa, Preparation of ultrafine jet-milled powders for Nd-Fe-B sintered magnets using hydrogenation–disproportionation–desorption–recombination and hydrogen Decrepitation processes, Appl. Phys. Lett. 103 (2) (2013) 022404, https://doi.org/10.1063/1.4813399.

[10] R.S. Sheridan, A.J. Williams, I.R. Harris, A. Walton, Improved HDDR processing route for production of anisotropic powder from sintered NdFeB type magnets, J. Magn. Magn. Mater. 350 (2014) 114–118, https://doi.org/10.1016/j.jmmm.2013.09.042.

[11] T. Horikawa, M. Yamazaki, M. Matsuura, S. Sugimoto, Recent Progress in the development of high-performance bonded magnets using rare earth–Fe Compounds, Sci. Technol. Adv. Mater. 22 (1) (2021) 729–747, https://doi.org/10.1080/14686996.2021.1944780.

[12] I. Poenaru, E.A. Patroi, D. Patroi, A. Iorga, E. Manta, HDDR as advanced processing method and recycling technology to address the rare-earth resource criticality in high performance Nd2Fe14B magnets production, J. Magn. Magn. Mater. 577 (2023) 170777, https://doi.org/10.1016/j.jmmm.2023.170777.

[13] P. Dalmas de Réotier, D. Fruchart, P. Wolfers, P. Vulliet, A. Yaouanc, R. Fruchart, P. L'Héritier, Properties of hydrided RE2Fe14B compounds, J. Phys. Colloq. 46 (C6) (1985) C6-249–C6-251, https://doi.org/10.1051/jphyscol:1985643.

[14] D. Book, I.R. Harris, Hydrogen absorption/desorption and HDDR studies on Nd16Fe76B8 and Nd11.8Fe82.3B5.9, J. Alloys Compd. 221 (1–2) (1995) 187–192, https://doi.org/10.1016/0925-8388(94)01433-7.

[15] J.M. Cadogan, J.M.D. Coey, Hydrogen absorption and desorption in Nd2Fe14B, Appl. Phys. Lett. 48 (6) (1986) 442–444, https://doi.org/10.1063/1.96525.

[16] V.A. Yartys, A.J. Williams, K.G. Knoch, P.J. McGuiness, I.R. Harris, Further studies of anisotropic hydrogen Decrepitation in Nd16Fe76B8 sintered magnets, J. Alloys Compd. 239 (1) (1996) 50–54, https://doi.org/10.1016/0925-8388(95)02185-X.

[17] M. Zakotnik, E. Devlin, I.R. Harris, A.J. Williams, Hydrogen Decrepitation and recycling of NdFeB-type sintered magnets, J. Iron Steel Res. Int. 13 (2006) 289–295, https://doi.org/10.1016/S1006-706X(08)60197-1.

[18] M.Z. Rasheed, S.-W. Nam, J.-Y. Cho, K.-T. Park, B.-S. Kim, T.-S. Kim, Review of the liquid metal extraction process for the recovery of Nd and Dy from permanent magnets, Metall. Mater. Trans. B Process Metall. Mater. Process. Sci. 52 (3) (2021) 1213–1227, https://doi.org/10.1007/s11663-021-02102-z.

[19] N. Stankovic, J. Jourdan, J. Marin, A. Chagnes, T. Quatravaux, Kinetic study of rare earth elements extraction from decrepitated magnet powder using liquid magnesium, RSC Adv. 13 (46) (2023) 32824–32832, https://doi.org/10.1039/D3RA05796H.

[20] M.K. Jha, A. Kumari, R. Panda, J. Rajesh Kumar, K. Yoo, J.Y. Lee, Review on hydrometallurgical recovery of rare earth metals, Hydrometallurgy 161 (2016) 77, https://doi.org/10.1016/j.hydromet.2016.01.003.

[21] J.W. Lyman, G.R. Palmer, Recycling of rare earths and Iron from NdFeB magnet scrap, High Temp. Mater. Processes 11 (1–4) (1993) 175–188, https://doi.org/10.1515/HTMP.1993.11.1-4.175.

[22] J.P. Rabatho, W. Tongamp, Y. Takasaki, K. Haga, A. Shibayama, Recovery of Nd and Dy from rare earth magnetic waste sludge by hydrometallurgical process, J. Mater. Cycles Waste Manag. 15 (2) (2013) 171–178, https://doi.org/10.1007/s10163-012-0105-6.

[23] H.-S. Yoon, C.-J. Kim, K. Chung, S. Jeon, I. Park, K. Yoo, M. Jha, The effect of grinding and roasting conditions on the selective leaching of Nd and Dy from NdFeB magnet scraps, Metals 5 (3) (2015) 1306–1314, https://doi.org/10.3390/met5031306.

[24] T. Vander Hoogerstraete, B. Blanpain, T. Van Gerven, K. Binnemans, From NdFeB magnets towards the rare-earth oxides: a recycling process consuming only oxalic acid, RSC Adv. 4 (109) (2014) 64099–64111, https://doi.org/10.1039/C4RA13787F.

[25] A. Kumari, M.K. Sinha, S. Pramanik, S.K. Sahu, Recovery of rare earths from spent NdFeB magnets of wind turbine: leaching and kinetic aspects, Waste Manag. 75 (2018) 486–498, https://doi.org/10.1016/j.wasman.2018.01.033.

[26] P.K. Parhi, T.R. Sethy, P.C. Rout, K. Sarangi, Separation and recovery of neodymium and praseodymium from permanent magnet scrap through the hydrometallurgical route, Sep. Sci. Technol. 51 (13) (2016) 2232–2241, https://doi.org/10.1080/01496395.2016.1200087.

[27] C. Erust, A. Akcil, A. Tuncuk, H. Deveci, E.Y. Yazici, A multi-stage process for recovery of neodymium (Nd) and dysprosium (Dy) from spent hard disc drives (HDDs), Miner. Process. Extr. Metall. Rev. 42 (2) (2019) 90–101, https://doi.org/10.1080/08827508.2019.1692010.

[28] P.K. Parhi, S.S. Behera, Leaching kinetics study of neodymium from the scrap magnet using acetic acid, Sep. Purif. Technol. 160 (2016) 59–66, https://doi.org/10.1016/j.seppur.2016.01.014.

[29] M. Gergoric, A. Barrier, T. Retegan, Recovery of rare-earth elements from neodymium magnet waste using glycolic, maleic, and ascorbic acids followed by solvent extraction, J. Sustain. Metall. 5 (1) (2019) 85–96, https://doi.org/10.1007/s40831-018-0200-6.

[30] M. Gergoric, C. Ravaux, B.-M. Steenari, F. Espegren, T. Retegan, Leaching and recovery of rare-earth elements from neodymium magnet waste using organic acids, Metals 8 (9) (2018) 721, https://doi.org/10.3390/met8090721.

[31] G. Reisdörfer, D. Bertuol, E.H. Tanabe, Recovery of neodymium from the magnets of hard disk drives using organic acids, Miner. Eng. 143 (2019) 105938, https://doi.org/10.1016/j.mineng.2019.105938.

[32] S. Belfqueh, A. Seron, S. Chapron, G. Arrachart, N. Menad, Evaluating organic acids as alternative leaching reagents for rare earth elements recovery from NdFeB magnets, J. Rare Earths 41 (4) (2023) 621–631, https://doi.org/10.1016/j.jre.2022.04.027.

[33] P.A. Vesilind, The rosin-Rammler particle size distribution, Resour. Recover. Conserv. 5 (3) (1980) 275–277, https://doi.org/10.1016/0304-3967(80)90007-4.

[34] M. Alderliesten, Mean particle diameters. Part VII. The rosin-rammler size distribution: physical and mathematical properties and relationships to moment-ratio defined mean particle diameters, Part. Part. Syst. Charact. 30 (3) (2013) 244–257, https://doi.org/10.1002/ppsc.201200021.

[35] M. Bonin, F.-G. Fontaine, D. Larivière, M. Bonin, F.-G. Fontaine, D. Larivière, Comparative studies of digestion techniques for the dissolution of neodymium-based magnets, Metals 11 (8) (2021), https://doi.org/10.3390/met11081149.

[36] W. Zhang, Z. Hu, Recent advances in sample preparation methods for elemental and isotopic analysis of geological samples, Spectrochim. Acta B At. Spectrosc. 160 (2019) 105690, https://doi.org/10.1016/j.sab.2019.105690.

[37] S. Mousavinezhad, S. Kadivar, E. Vahidi, Comparative life cycle analysis of critical materials recovery from spent Li-ion batteries, J. Environ. Manag. 339 (2023) 117887, https://doi.org/10.1016/j.jenvman.2023.117887.

[38] R.G. Pearson, Hard and soft acids and bases, J. Am. Chem. Soc. 85 (22) (1963) 3533–3539, https://doi.org/10.1021/ja00905a001.

[39] R.G. Pearson, Hard and soft acids and bases, HSAB, Part 1: fundamental principles, J. Chem. Educ. 45 (9) (1968) 581, https://doi.org/10.1021/ed045p581.

[40] D.D. Wagman, W.H. Evans, V.B. Parker, R.H. Schumm, I. Halow, S.M. Bailey, K. L. Churney, R.L. Nuttall, Erratum: the NBS tables of chemical thermodynamic properties. Selected values for inorganic and C1 and C2 organic substances in SI units [J. Phys. Chem. Ref. data 11, Suppl. 2 (1982)], J. Phys. Chem. Ref. Data Monogr. 18 (4) (1989) 1807–1812, https://doi.org/10.1063/1.555845.

[41] S. Kappenthuler, S. Olveira, J. Wehrli, S. Seeger, Environmental assessment of alternative Methanesulfonic acid production using direct activation of methane, J. Clean. Prod. 202 (2018) 1179–1191, https://doi.org/10.1016/j.jclepro.2018.07.284.

[42] I.S. Modahl, A. Brekke, The 2019 LCA of products from Borregaard, Sarpsborg; OR.14.21; Norwegian Institute for Sustainability Research (NORSUS): Fredrikstad, Norway. https://norsus.no/en/publikasjon/the-2019-lca-of-products-from-borregaard-sarpsborg/, 2021.

[43] P.K. Parhi, K.H. Park, C.W. Nam, J.T. Park, Liquid-liquid extraction and separation of Total rare earth (RE) metals from polymetallic manganese nodule leaching solution, J. Rare Earths 33 (2) (2015) 207–213, https://doi.org/10.1016/S1002-0721(14)60404-X.

[44] M. Mohammadi, K. Forsberg, L. Kloo, J. Martinez De La Cruz, Å. Rasmuson, Separation of ND(III), DY(III) and Y(III) by solvent extraction using D2EHPA and EHEHPA, Hydrometallurgy 156 (2015) 215–224, https://doi.org/10.1016/j.hydromet.2015.05.004.

[45] F. Xie, T.A. Zhang, D. Dreisinger, F. Doyle, A critical review on solvent extraction of rare earths from aqueous solutions, Miner. Eng. 56 (2014) 10–28, https://doi.org/10.1016/j.mineng.2013.10.021.

[46] V. Jedináková, P. Vaňura, J. Žilková, V. Bílek, F. Touati, Extraction of Micro- and macroconcentrations of rare earth ions with the mixture of D2EHPA and TBP in n-hexane and cyclohexane, J. Radioanal. Nucl. Chem. 162 (2) (1992) 267–276, https://doi.org/10.1007/BF02035387.
[47] J. Kraikaew, W. Srinuttrakul, C. Chayavadhanakur, Solvent extraction study of rare earths from nitrate medium by the mixtures of TBP and D2EHPA in kerosene, J. Metals Mater. Minerals 15 (2) (2005) 89–95.
[48] D.F. Peppard, J.P. Faris, P.R. Gray, G.W. Mason, Studies of the solvent extraction behavior of transition elements. I. Order and degree of fractionation of the trivalent rare earths, J. Phys. Chem. 57 (3) (1953) 294–301, https://doi.org/10.1021/j150504a008.
[49] P.I. Matveev, V.G. Petrov, B.V. Egorova, N.N. Senik, A.S. Semenkova, O. V. Dubovaya, A.V. Valkov, S.N. Kalmykov, Solvent extraction of rare earth elements by tri-*n*-butyl phosphate and tri-Iso-amyl phosphate in the presence of ca (NO3)2, Hydrometallurgy 175 (2018) 218–223, https://doi.org/10.1016/j.hydromet.2017.12.007.
[50] M.-S. Lee, G.-S. Lee, K.Y. Sohn, Solvent extraction equilibria of FeCl3 with TBP, Mater. Trans. 45 (6) (2004) 1859–1863, https://doi.org/10.2320/matertrans.45.1859.
[51] R. Lommelen, B. Dewulf, J. Bussé, K. Binnemans, Predictive thermodynamic model for solvent extraction of Iron(III) by tri-*n*-butyl phosphate (TBP) from chloride media, Sep. Purif. Technol. 348 (2024) 127708, https://doi.org/10.1016/j.seppur.2024.127708.
[52] T.R. Bhat, S. Sundararajan, The extraction of Gallium chloride by Tributyl phosphate and the recovery of gallium from Bayer liquor, J. Less Common Metals 12 (3) (1967) 231–238, https://doi.org/10.1016/0022-5088(67)90118-X.
[53] A. Fortuny, M.T. Coll, C.S. Kedari, A.M. Sastre, Effect of phase modifiers on boron removal by solvent extraction using 1,3 Diolic Compounds, J. Chem. Technol. Biotechnol. 89 (6) (2014) 858–865, https://doi.org/10.1002/jctb.4322.
[54] R. Banda, S.H. Sohn, M.S. Lee, Solvent extraction separation of Mo and co from chloride solution containing Al, Mater. Trans. 54 (1) (2013) 61–65, https://doi.org/10.2320/matertrans.M2012287.
[55] N.A. Grigorieva, I.Yu. Fleitlikh, O.A. Logutenko, T.Yu. Ivanenko, S.A. Novikova, Scandium extraction from sulfate media with Di-(2-Ethylhexyl) phosphoric acid in Decane or toluene mixed with proton-donor additives, Hydrometallurgy 232 (2025) 106435, https://doi.org/10.1016/j.hydromet.2024.106435.
[56] R.R. Varela, A. Chagnes, K. Forsberg, R.R. Varela, A. Chagnes, K. Forsberg, Third-phase formation in rare earth element extraction with D2EHPA: key factors and impact on liquid membrane extraction performance, Membranes 15 (7) (2025), https://doi.org/10.3390/membranes15070188.
[57] L.S. Maslennikova, O.A. Sinegribova, Extraction of Gd, Tb, and Dy from nitrate media with a mixture of technical Di-2-Ethylhexyl phosphoric acid and Tributylphosphate, Theor. Found. Chem. Eng. 51 (5) (2017) 850–857, https://doi.org/10.1134/S0040579517050153.
[58] M. Gergoric, C. Ekberg, B.-M. Steenari, T. Retegan, Separation of heavy rare-earth elements from light rare-earth elements via solvent extraction from a neodymium magnet leachate and the effects of diluents, J. Sustain. Metall. 3 (3) (2017) 601–610, https://doi.org/10.1007/s40831-017-0117-5.
[59] C.K. Gupta, N. Krishnamurthy, Extractive Metallurgy of Rare Earths, CRC Press, Boca Raton. - References - Scientific Research Publishing, 2005. https://www.scirp.org/reference/referencespapers?referenceid=2189105. (Accessed 10 December 2025).
[60] K.L. Nash, A review of the basic chemistry and recent developments in trivalent F-elements separations, Solvent Extr. Ion Exch. 11 (4) (1993) 729–768, https://doi.org/10.1080/07366299308918184.
[61] H.-S. Yoon, C.-J. Kim, K.W. Chung, S.-D. Kim, J.R. Kumar, Recovery process development for the rare earths from permanent magnet scraps leach liquors, J. Braz. Chem. Soc. 26 (2015) 1143–1151, https://doi.org/10.5935/0103-5053.20150077.
[62] A. Battsengel, A. Batnasan, K. Haga, A. Shibayama, Selective separation of light and heavy rare earth elements from the pregnant leach solution of apatite ore with D2EHPA, JMMCE 06 (05) (2018) 517–530, https://doi.org/10.4236/jmmce.2018.65037.
[63] H.-S. Yoon, C.-J. Kim, K.-W. Chung, S.-D. Kim, J.-Y. Lee, J.R. Kumar, Solvent extraction, separation and recovery of dysprosium (Dy) and neodymium (Nd) from aqueous solutions: waste recycling strategies for permanent magnet processing, Hydrometallurgy 165 (2016) 27–43, https://doi.org/10.1016/j.hydromet.2016.01.028.
[64] G. Zhang, D. Chen, G. Wei, H. Zhao, L. Wang, T. Qi, F. Meng, L. Meng, Extraction of Iron (III) from chloride leaching liquor with high acidity using tri-n-butyl phosphate and synergistic extraction combined with methyl isobutyl ketone, Sep. Purif. Technol. 150 (2015) 132–138, https://doi.org/10.1016/j.seppur.2015.07.001.
[65] F. Habashi, in: Fathi Habashi (Ed.), Handbook of Extractive Metallurgy, Volume 2, 1997.
[66] A. Klemettinen, Z. Adamski, I. Chojnacka, A. Leśniewicz, L. Rycerz, Recovery of rare earth elements from the leaching solutions of spent NdFeB permanent magnets by selective precipitation of rare earth oxalates, Minerals 13 (7) (2023), https://doi.org/10.3390/min13070846.
[67] S. Ilyas, R. Ranjan Srivastava, H. Kim, Solvent extraction for high separation strategy of light and heavy rare earth elements from a sulfate-leached solution of low-grade monazite, Sep. Purif. Technol. 341 (2024) 126896, https://doi.org/10.1016/j.seppur.2024.126896.
[68] K.N. Han, Characteristics of precipitation of rare earth elements with various precipitants, Minerals 10 (2) (2020), https://doi.org/10.3390/min10020178.
[69] R. Chi, Z. Xu, A solution chemistry approach to the study of rare earth element precipitation by oxalic acid, Metall. Mater. Trans. B Process Metall. Mater. Process. Sci. 30 (2) (1999) 189–195, https://doi.org/10.1007/s11663-999-0047-0.
[70] U.S. Department of Energy, Critical minerals and materials: U.S. *Department of Energy's Strategy to Support Domestic Critical Mineral and Material Supply Chains (FY 2021–FY 2031)*; Office of Energy Efficiency and Renewable Energy: Washington, DC, USA. https://www.energy.gov/sites/prod/files/2021/01/f82/DOE%20Critical%20Minerals%20and%20Materials%20Strategy_0.pdf, 2021.
[71] A. Schreiber, J. Marx, P. Zapp, W. Kuckshinrichs, Comparative life cycle assessment of neodymium oxide electrolysis in molten salt, Adv. Eng. Mater. 22 (6) (2020) 1901206, https://doi.org/10.1002/adem.201901206.
[72] Y. Zhu, J. Li, D. Xie, H. Zhang, M. Li, B. Xu, X. Zhang, Y. Xie, T. Qi, Aluminum removal from rare earth chloride solution through regulated hydrolysis via electrochemical method, Separations 11 (5) (2024), https://doi.org/10.3390/separations11050149.
[73] J.-Y. Lin, Y.-J. Shih, P.-Y. Chen, Y.-H. Huang, Precipitation recovery of boron from aqueous solution by chemical Oxo-precipitation at room temperature, Appl. Energy 164 (2016) 1052–1058, https://doi.org/10.1016/j.apenergy.2014.12.058.
[74] A. Kumari, S.K. Sahu, A comprehensive review on recycling of critical raw materials from spent neodymium Iron boron (NdFeB) magnet, Sep. Purif. Technol. 317 (2023) 123527, https://doi.org/10.1016/j.seppur.2023.123527.
[75] H. Zheng, Y. Ding, S. You, Y. Ding, S. Zhang, J. Zhang, A comprehensive review of neodymium-Iron-boron (NdFeB) waste recycling: processes, mechanisms, and prospects, J. Environ. Manag. 391 (2025) 126513, https://doi.org/10.1016/j.jenvman.2025.126513.